

# Compact Objects in EsGB Theory and beyond

Panagiota Kanti

Theory Division, Physics Department, University of Ioannina,  
Ioannina GR 451 10, Greece  
pkanti@uoi.gr

**Abstract.** In the context of General Relativity, black holes are not allowed to possess scalar hair, wormholes are not traversable and particle-like solutions are irregular. Therefore, in order to derive novel and physically interesting solutions that describe compact objects one needs to address generalised gravitational theories. One popular class of such theories is the Einstein-scalar-Gauss-Bonnet (EsGB) theory with a general coupling function between the scalar field of the theory and the quadratic Gauss-Bonnet term. Starting from black holes, we present a variety of spherically-symmetric solutions for several different forms of the coupling function and discuss their main features. We then proceed to wormhole solutions and demonstrate that the EsGB theory naturally supports traversable wormholes without the need for exotic matter. Regular scalarised particle-like solutions also emerge in the context of the same theory which also possess interesting observable features such as photon rings and echoes. Moving beyond this class of theories, we then address the more extended scalar-tensor Horndeski theory, briefly mention the types of black-hole solutions that arise, and demonstrate that an appropriately constructed disformal transformation of a black-hole solution, such as the Lu-Pang solution, results into a traversable wormhole in the context of the beyond-Horndeski theory.

**Keywords:** Einstein-scalar-Gauss-Bonnet theory, black holes, wormholes, particle-like solutions, Horndeski theory

## 1 Introduction

In 1915, Albert Einstein formulated the General Theory of Relativity [1], a mathematically beautiful and, at the same time, a physically relevant theory which has so far passed all experimental tests. It is, in addition, a much more interesting theory compared to Newtonian Gravity since, not only does it describe the gravitational interactions between two massive bodies, but it also incorporates the equivalence between mass and energy, and proceeds further to predict the existence of new gravitational solutions, such as black holes or wormholes, and new phenomena associated with them.

However, General Relativity (GR) is not a perfect theory – if such a thing ever exists. On the cosmological side, the Standard Cosmological Model, which has been formulated on the mathematical and physical basis provided by GR,

has a number of open problems: the nature of dark matter and dark energy, the coincidence problem, the spacetime singularities, the right model for inflation, to mention a few. Also, the prospect of the unification of gravity with the other forces seems unlikely within the GR – the latter theory is a tensorial theory rather than a gauge field theory, and is not renormalizable. But even on the gravitational side, GR is a rather restricted theory predicting in fact the existence of a limited number of types of compact objects beyond stars, some of them with undesirable properties: black holes obey “no-hair” theorems, wormholes cannot keep their tunnels open or are plagued by internal singularities and gravitational particle-like solutions (solitons) simply do not exist.

Therefore, in order to find new black-hole solutions, traversable wormholes or particle-like solutions, going beyond General Relativity seems to be a one-way road. For this reason, a large number of generalised theories of gravity have been formulated by adding to the Einstein-Hilbert action new fields, new gravitational terms and couplings among them. The simplest extension of GR is the scalar-tensor theories [2]-[6], however, as it quite well known, one must consider non-minimally coupled scalar fields in order for physically-interesting solutions to emerge.

In this review, we will focus first on the Einstein-scalar-Gauss-Bonnet (EsGB) theory as an indicative example of a non-minimal-coupled scalar-tensor theory. It is a rather simple theory containing a single scalar degree of freedom coupled to the quadratic, gravitational Gauss-Bonnet term. This theory has been studied for decades, as it arises in the context of superstring effective theory at low energies [7]-[9] or in Kaluza-Klein compactifications of Lovelock’s theory [10]. Due to the presence of the quadratic Gauss-Bonnet (GB) term, this generalised theory reduces to GR, with a trivial scalar field, in the limit of weak gravity but may lead to important modifications from GR in the strong-gravity regime. These modifications include novel gravitational solutions characterised by a non-trivial scalar field. Thus, in the context of the EsGB theory, we will search for new scalarised solutions describing various types of compact objects. As we will demonstrate, the configuration space of solutions of the EsGB theory is indeed a particularly rich one, with some areas of it still waiting to be explored.

The EsGB theory is in fact a subclass of Horndeski theory [11], which is a the most general scalar-tensor theory with field equations containing only up to 2nd order derivatives of the metric tensor and the scalar field. The scalar field is now allowed to have a number of couplings with different gravitational terms and derivative-like couplings as well. The theory can be further generalised to the beyond-Horndeski theory via the addition of two additional terms in the Lagrangian. In the second part of this review, we will focus on the beyond-Horndeski theory, and demonstrate that, in its context, new solutions describing black holes with an (Anti-)de Sitter-Reissner-Nordstrom asymptotic behaviour at large distances may be analytically derived. For the derivation of wormhole solutions, we will employ an alternative method, that of applying a disformal transformation to a known solution of the theory. We will show that such an

approach can easily lead to new wormhole solutions with a number of particularly attractive properties.

The outline of this review is as follows: in Section 2, we will give a brief overview of the type of compact objects arising in the context of GR and of the minimal Einstein-scalar theory. In Section 3, we will present the EsGB theory, and search for black holes, wormholes and particle-like solutions in its context. In Section 4, we will proceed to consider the beyond-Horndeski theory, and present some recent results on black holes and wormhole solutions. We will present our conclusions and some food-for-thought comments for the future in Section 5.

## 2 Compact Objects in GR and Einstein-scalar theory

In this section, we will briefly discuss the main characteristics of three types of compact objects that will be of interest to us, namely black holes, wormholes and particle-like solutions, as these arise in the context of General Relativity and Einstein-scalar theory.

### 2.1 Black Holes

As is well known, General Relativity admits only three families of black-hole solutions: the Schwarzschild solution [12], which describes a spherically-symmetric, neutral black hole, the Reissner-Nordstrom solution [13], which also describes a spherically-symmetric but charged black hole, and the Kerr(-Newman) solution [14], which describes a rotating, neutral (or, charged) black hole. According to the “no-hair” theorems of GR [15], a BH may be characterized at most by only three parameters – three physical, conserved quantities – namely its mass  $M$ , electromagnetic charge  $Q$  and angular-momentum  $J$ . All three aforementioned GR solutions perfectly comply with this dictation.

The simplest extension of pure General Relativity amounts to the addition of a free, massless scalar field  $\phi$  to the theory. If we assume that this field is a static, spherically-symmetric one, i.e.  $\phi = \phi(r)$ , its equation of motion simply reads

$$\square\phi = 0 \Rightarrow \partial_r[\sqrt{-g}g^{rr}\partial_r\phi] = 0. \quad (1)$$

For an invertible metric tensor with  $g \neq 0$ , the above leads to the result

$$\phi' \sim g_{rr}, \quad (2)$$

which diverges at the horizon. As a result, the simple Einstein-scalar theory does not possess a regular, scalarised black-hole solution.

Even for a self-interacting scalar field with  $V(\phi) \neq 0$ , Bekenstein’s *old scalar “no-hair theorem”* [15] excludes regular black-hole solutions in a general class of minimally-coupled scalar-tensor theories. Starting from the scalar-field equation, multiplying with  $\phi$ , integrating over the exterior spacetime, and performing an integration by parts of the  $\square\phi$  term, we obtain [16]

$$\int_{\mathcal{V}} d^4x \sqrt{-g} [\partial_\mu\phi \partial^\mu\phi + \phi V'(\phi)] + \int_{\partial\mathcal{V}} d^3x \sqrt{h} \eta^\mu \phi \partial_\mu\phi = 0. \quad (3)$$

The boundary term at the end of the above expression vanishes both at the horizon of the black hole, provided that the scalar field remains there finite, and at asymptotic infinity, under the assumption that the self-interacting scalar field falls off sufficiently fast. The first term inside brackets gives  $g^{rr}(\partial_r\phi)^2 > 0$  and, thus, the constraint allows for scalarised black-hole solutions only in the case where  $\phi V'(\phi) < 0$ . However, for e.g. a typical mass term  $V(\phi) = m^2\phi^2/2$ , this would demand  $m^2 < 0$  and would result in a non-physical theory. Generalising this, we may therefore conclude that any theory with a minimally-coupled scalar field and a self-interacting potential satisfying the constraint  $\phi V'(\phi) > 0$  does not allow for black-hole solutions with a non-trivial, static scalar hair.

## 2.2 Wormholes

General Relativity admits a second class of compact objects, namely wormholes, which are in fact hidden in the interior of all black-hole solutions that the theory predicts. Unfortunately, these wormhole solutions are not *traversable*.

Taking the Schwarzschild black-hole line-element as a paradigm

$$ds^2 = -\left(1 - \frac{2M}{r}\right) dt^2 + \left(1 - \frac{2M}{r}\right)^{-1} dr^2 + r^2 (d\theta^2 + \sin^2\theta d\varphi^2), \quad (4)$$

it is clear that whereas the exterior region ( $r > 2M$ ) of this background is clearly static, the interior region ( $r < 2M$ ), due to the change of its signature as we cross the horizon, is clearly dynamical. Even the presence of the spacetime singularity at  $r = 0$  is not in fact a static feature of the complete Schwarzschild spacetime. A simple but careful analysis [17] reveals that, as the time goes by, a throat appears in the place of the singularity, which connects two asymptotically far-away regions. The radius of the throat expands, reaches its maximum value  $r_{max} = 2M$  and then shrinks again and disappears leaving behind the two spacetime singularities of the black and the white hole which together comprise the complete Schwarzschild geometry. Unfortunately, this Einstein-Rosen passage [18][19][20] opens and closes so quickly that no physical particles, including photons, can pass through.

The Reissner-Nordstrom and Kerr geometries also possess similar internal tunnels. In fact, due to the presence of the internal Cauchy horizons in both of these solutions, the spacetime singularity can always be avoided and the tunnel remains always open. Unfortunately, it is again non-traversable: the internal Cauchy horizons they both possess are unstable, and any small disturbance causes them to collapse and turns them to a spacetime singularity, which unavoidably blocks the passage.

Trying to construct a more general theory than GR, in the context of which a traversable wormhole solution could emerge, we may add as before a scalar field, free of self-interacting. One could also adopt a different perspective [21] on how the spacetime should look like in order to avoid altogether the presence of a horizon or a spacetime singularity, thus enhancing the probability for constructing a traversable wormhole. As we will see in detail in Section 4, where we will

also follow this different perspective, the addition of a massless scalar field can indeed support a wormhole solution, the well-known Ellis-Bronnikov wormhole [22][23]. However, the scalar field must be a *ghost* one since its energy density  $\rho$  satisfies the constraint  $\rho < 0$ , and thus violates the energy conditions. The addition of a self-interacting potential also leads to constraints on the energy density and pressure components of the theory which again hint to some exotic form of matter rather than a physical field.

### 2.3 Particle-like solutions

In flat Minkowski spacetime, solutions that are regular and describe different types of distribution of matter are quite common, and are usually termed *solitons*. However, in the context of a pure gravitational theory, such as General Relativity, no such regular solutions emerge.

The same conclusion holds when simple modifications of GR are considered. For instance, if we add again a massless, spherically-symmetric scalar field to the theory, the well-known Fisher/Janis-Newman-Winicour-Wyman solution [24]-[26] can be found where the metric components and scalar field are given by the expressions

$$|g_{tt}| \sim (r - r_s)^{2s}, \quad g_{rr} \sim (r - r_s)^{2(1-s)}, \quad \phi \sim D \ln(r - r_s), \quad (5)$$

respectively, with  $s = 1/\sqrt{1 + (D/2M)^2}$ . In the above,  $M$  is the mass of the solution and  $D$  a scalar “charge”. However, as one may see by calculating the gravitational scalar quantities of the spacetime, this is an irregular solution since the latter diverge at the radius  $r_s = M/2s$ . Similar results follow if one adds a self-interacting potential for the scalar field.

## 3 The Einstein-Scalar-GB Theory

According to the brief review of compact objects presented in Section 2, one would need to consider a theory beyond pure GR as well as beyond the simple Einstein-scalar theory in order to discover novel solutions describing compact objects which are physically interesting. A more elaborate, generalised theory of gravity could follow by introducing extra fields and/or higher gravitational terms, and could be schematically described by the following action functional

$$S = \int d^4x \sqrt{-g} \left[ f(R, R_{\mu\nu}, R_{\mu\nu\rho\sigma}, \Phi_i) + \mathcal{L}_X(\Phi_i) \right], \quad (6)$$

where  $R_{\mu\nu\rho\sigma}$  is the Riemann tensor,  $R_{\mu\nu}$  the Ricci tensor,  $R$  the Ricci scalar and  $\Phi_i$  stands collectively for the different types of fields present in the theory whose properties are described by the Lagrangian  $\mathcal{L}_X(\Phi_i)$ . In what follows, we will retain, apart from the gravitational field, a single additional, scalar degree of freedom and ignore all other forms of fields. We will nevertheless introduce a higher-derivative term in the form of a quadratic gravitational term. Such a

term would naturally go unnoticed in regions of weak gravitational field but could cause significant deviations from GR in the strong field regime.

In particular, we will consider the following generalised, quadratic theory of gravity

$$S = \int d^4x \sqrt{-g} \left[ \frac{R}{16\pi G} - \frac{1}{2} \partial_\mu \phi \partial^\mu \phi + f(\phi) R_{GB}^2 \right], \quad (7)$$

where  $R_{GB}^2$  is the so-called Gauss-Bonnet (GB) term

$$R_{GB}^2 = R_{\mu\nu\rho\sigma} R^{\mu\nu\rho\sigma} - 4R_{\mu\nu} R^{\mu\nu} + R^2 \quad (8)$$

and  $f(\phi)$  is an arbitrary coupling function between the scalar field  $\phi$  and the GB term. The above theory is hardly a new one – in fact, it is common knowledge that it arises as part of the string effective action at low energies, as part of a Lovelock effective theory in four dimensions or as part of an extended scalar-tensor (Horndeski or DHOST) theory. It is a higher-derivative, gravitational theory of gravity yet simpler than one would expect: the particular combination of the gravitational quantities appearing in the definition of the GB term (8) guarantees that the field equations contain only up to 2nd-order derivatives of the metric tensor and the scalar field thus avoiding any Ostrogradski instabilities [27]. It is in the context of this quadratic theory – upgraded to a class of theories due to the general form of the coupling function  $f(\phi)$  – that we will look for scalarised solutions describing novel black-holes, traversable wormholes and regular particle-like solutions.

### 3.1 Black-Hole Solutions in Einstein-Scalar-GB Theory

Do we have any reason to believe that the generalised gravitational theory (7) may lead to scalarised black holes, in other words that this theory violates Bekenstein’s scalar no-hair theorem? Yes, quite a few indeed. To start with, more than 25 years ago, a novel type of black holes, the so-called *dilatonic* black holes [28][29], were discovered in the context of the theory (7) with an exponential coupling function, i.e.  $f(\phi) = \alpha e^\phi$ , between the scalar field, or dilaton, and the GB term. Due to the presence of the GB term, the field equations are quite complicated and cannot be solved analytically - therefore, the dilatonic black holes, as well as a large number of variants of this solution were found either in an approximate form or through numerical integration (see [30]-[47] for an indicative list of works).

Two decades later, another class of scalarised black-hole solutions was found [48][49] in the context of the shift-symmetric EsGB theory, i.e. for the choice  $f(\phi) = \alpha\phi$  of the coupling function. Here, as in the case of the dilatonic black holes, too,  $\alpha$  is a coupling constant of the theory. Both the dilatonic and the scalarised shift-symmetric black-hole solutions violated the requirements of the scalar no-hair theorems, both the old [15] and the new versions [50][51][52] of it, thus paving the way for new black-hole solutions with characteristics not allowed by General Relativity [53][54].

The obvious question which readily emerges is whether we can find additional classes of black-hole solutions in the context of the theory (7) but for other choices of the coupling function apart from the exponential and the linear one. To investigate this, we reconsidered the Einstein-scalar-GB theory but allowed for a general form of the coupling function  $f(\phi)$  [55][56]. We focused on the simplest possible background, that of a static, spherically-symmetric black hole, and assumed the following form of line-element

$$ds^2 = -e^{A(r)} dt^2 + e^{B(r)} dr^2 + r^2(d\theta^2 + \sin^2 \theta d\varphi^2), \quad (9)$$

with two unknown metric functions of the radial coordinate. Taking the variation of the action (7) with respect to the scalar field  $\phi$  and the metric tensor  $g_{\mu\nu}$ , we obtain the scalar field and gravitational field equations

$$\nabla^2 \phi + \dot{f}(\phi) R_{GB}^2 = 0, \quad R_{\mu\nu} - \frac{1}{2} g_{\mu\nu} R = T_{\mu\nu}, \quad (10)$$

respectively. In the above

$$T_{\mu\nu} = -\frac{1}{4} g_{\mu\nu} (\partial\phi)^2 + \frac{1}{2} \partial_\mu \phi \partial_\nu \phi - \frac{1}{2} (g_{\rho\mu} g_{\lambda\nu} + g_{\lambda\mu} g_{\rho\nu}) \eta^{\kappa\lambda\alpha\beta} \tilde{R}^{\rho\gamma}{}_{\alpha\beta} \nabla_\gamma \partial_\kappa f \quad (11)$$

is the energy-momentum tensor of the theory which receives contributions from both the kinetic term of the scalar field and its non-minimal coupling to the quadratic GB term.

The set of field equations (10) involve the two unknown metric functions  $A(r)$  and  $B(r)$ , and the scalar field  $\phi(r)$ . In fact, the  $(rr)$ -component of the gravitational equations takes the form of a 2nd order polynomial for  $e^B$ , which therefore may be determined once the solutions for  $A(r)$  and  $\phi(r)$  are found. The remaining equations reduce indeed to a system of only two independent, ordinary differential equations of second order for the unknown functions  $A(r)$  and  $\phi(r)$ , which is given below schematically

$$A'' = \frac{P}{S}, \quad \phi'' = \frac{Q}{S}. \quad (12)$$

The quantities  $(P, Q, S)$  depend on  $(r, \phi, \phi', A')$ , and the interested reader may find their exact expressions as well as the remaining technical details of this analysis in [55][56].

Due to the complexity of the quantities involved, the integration of the system demands numerical integration. However, it may be solved analytically in the small and large regimes of the radial coordinate. The corresponding solutions may be used as boundary solutions for the general solution of the system and, in addition, their form will reveal under which constraints these describe indeed a robust black-hole background.

Starting from the small  $r$ -regime, we demand the presence of the most important feature of black-hole geometry, that of a regular horizon. For this, we impose the asymptotic behaviour

$$e^{A(r)} \rightarrow 0, \quad e^{-B(r)} \rightarrow 0, \quad \phi(r) \rightarrow \phi_h, \quad (13)$$

as  $r$  approaches a certain value  $r_h$ . The last demand – the finiteness of the scalar field – encompasses the notion of the regularity of the black-hole horizon. The same must naturally hold for the first and second derivative of the field. However, demanding that, under the behaviour of the metric functions displayed in (13),  $\phi''$  remains finite at the horizon  $r_h$ , the second of the equations in (12) leads to the constraint

$$\phi'_h = \frac{r_h}{4f_h} \left( -1 \pm \sqrt{1 - \frac{96\dot{f}_h^2}{r_h^4}} \right). \quad (14)$$

The above formula ensures that, for a selected coupling function and value of the scalar field  $\phi_h$  at the black-hole horizon  $r_h$ , choosing this particular value for  $\phi'_h$  leads to a gravitational background that describes the near-horizon geometry of a black hole. No constraint arises on the form of the coupling function  $f(\phi)$  itself, which therefore remains arbitrary. The coupling function needs to satisfy an additional constraint which follows from the positivity of the expression under the square root in (14); this may be written as

$$\dot{f}_h^2 < \frac{r_h^4}{96}, \quad (15)$$

and interpreted as a bound on the lower value of the black-hole horizon radius  $r_h$  for a given  $f(\phi)$  and  $\phi_h$ . It is this characteristic that distinguishes the GB black hole from the Schwarzschild black hole, its analog in the context of GR. Using the above results, the field equations may give the asymptotic forms of the metric functions and scalar field near the horizon, which are found to have the form

$$e^A = a_1(r - r_h) + \dots, \quad e^{-B} = b_1(r - r_h) + \dots, \quad (16)$$

$$\phi = \phi_h + \phi'_h(r - r_h) + \phi''_h(r - r_h)^2 + \dots, \quad (17)$$

At the other asymptotic regime, i.e. at large distances from the horizon, we assume, as usually, a power series expansion in  $1/r$  for the three unknown functions, namely

$$e^A = 1 + \sum_{n=1}^{\infty} \frac{p_n}{r}, \quad e^B = 1 + \sum_{n=1}^{\infty} \frac{q_n}{r}, \quad \phi = \phi_{\infty} + \sum_{n=1}^{\infty} \frac{d_n}{r}. \quad (18)$$

Substituting these expressions into the field equations, we may determine the arbitrary coefficients  $(p_n, q_n, d_n)$ . In fact,  $p_1$  and  $d_1$  remain arbitrary and are identified with the black-hole mass  $M$  and scalar charge  $D$ , respectively. The asymptotic form of the metric and scalar field then take the final form

$$e^A = 1 - \frac{2M}{r} + \frac{MD^2}{12r^3} + \dots, \quad e^B = 1 + \frac{2M}{r} + \frac{16M^2 - D^2}{4r^2} + \dots, \quad (19)$$

$$\phi = \phi_{\infty} + \frac{D}{r} + \frac{MD}{r^2} + \frac{32M^2D - D^3}{24r^3} + \frac{12M^3D - 24M^2\dot{f} - MD^3}{6r^4} + \dots \quad (20)$$



As in the near-horizon analysis, no constraint on  $f(\phi)$  arises by demanding a robust black-hole geometry at large distances. A general coupling function  $f$  does not interfere with the existence of an asymptotically-flat limit with its exact form making an appearance not earlier than in the 4th order term of the expansion.

In order to construct a complete black-hole solution, we need to find a solution of the field equations (12) which smoothly interpolates between the two asymptotic forms (17) and (20). And this is where the no-hair theorems play a crucial role: if the theory (7) satisfies the requirements of the no-hair theorems, these dictate that no solution that smoothly connects these two asymptotic forms can be found. Let us look briefly into this. We will start from the old no-hair theorem and follow a similar analysis [15] [16]. We will employ the scalar-field equation, multiply by  $f(\phi)$  in our case, and integrate over the entire exterior spacetime. Performing an integration by parts, we arrive at the constraint [55][56][57]

$$\int_{\mathcal{V}} d^4x \sqrt{-g} \dot{f}(\phi) [\partial_\mu \phi \partial^\mu \phi - f(\phi) R_{GB}^2] - \int_{\partial\mathcal{V}} d^3x \sqrt{h} \eta^\mu f(\phi) \partial_\mu \phi = 0. \quad (21)$$

Due to the dependence of the scalar field solely on the radial coordinate, it holds that  $\partial_\mu \phi \partial^\mu \phi = g^{rr} (\partial_r \phi)^2 > 0$  and  $\eta^\mu \partial_\mu \phi = g^{rr} \partial_r \phi$ . The whole boundary term at the end of the above expression vanishes as usual at the black-hole horizon. However, as noted in [57], its value at asymptotic infinity depends on the form of the coupling function. If  $f(\phi_\infty) = 0$ , then the boundary term vanishes altogether and we need to address only the expression inside the square brackets in the first integral. One may easily see, by using the asymptotic expressions (17) and (20), that the GB term takes on positive values at the two asymptotic regimes [55][56] – as the exact numerical analysis reveals, in fact it remains positive over the entire exterior regime. Therefore, the emergence of black-hole solutions in this case is allowed only for  $f(\phi) > 0$  according to the old no-hair theorem. If, on the other hand,  $f(\phi_\infty) \neq 0$ , then the boundary term at asymptotic infinity reduces to  $f(\phi_\infty)D$ . In this case, solutions arise again for  $f(\phi) > 0$  but also for a certain interval for negative values of  $f(\phi)$  [57].

Let us now turn to Bekenstein's new version of no-hair theorem [50], developed for a theory with a minimally-coupled scalar field, and examine in turn whether the theory (7) evades its own requirements, too. This theorem relies on the particular profile of the  $T^r_r$  component of the energy-momentum tensor. For instance, it demands that, at asymptotic infinity,  $T^r_r$  is positive and decreasing. Indeed, using the asymptotic solution (20), and the exact expression of  $T^r_r$ , we find that this is indeed the case. Our result therefore agrees with the one derived in [50] at large distances; this was anticipated since the quadratic GB term is not expected to play any role far away from the black-hole horizon where the curvature of spacetime is small. In the near-horizon regime, the novel no-hair theorem dictates that  $T^r_r$  is negative and increasing. In the context of the Einstein-scalar-GB theory, though, this does not hold any more: indeed, if we use the near-horizon asymptotic solution (17), we find that

$$\text{sign}(T^r_r)_h = -\text{sign}(\dot{f}_h \phi'_h) = 1 \mp \sqrt{1 - 96 \dot{f}^2 / r_h^4}, \quad (22)$$

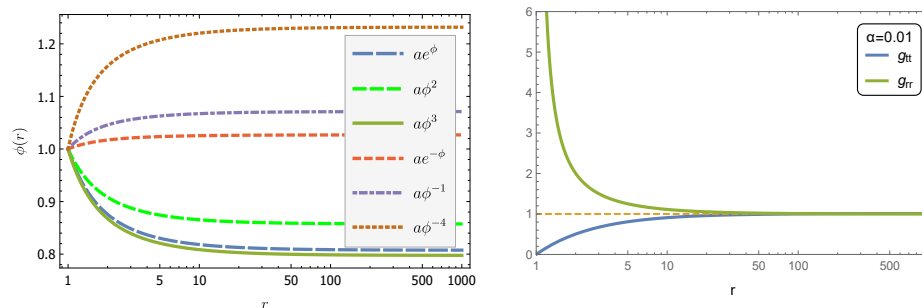


**Fig. 1.** The profile of the scalar field for a variety of choices for the coupling function  $f(\phi)$  (left plot), and the two metric functions (in absolute value, right plot) [55][56].

where we have used the constraint Eq. (14) for the regularity of the horizon. It is clear that the above expression is always positive-definite, in contrast to the requirement of the novel no-hair theorem. The presence of the GB term near the horizon – where the curvature is strong – changes the profile of  $T^r_r$ , and causes the evasion of Bekenstein’s new no-hair theorem.

The aforementioned argument was followed also in [28] to prove that the dilatonic theory with  $f(\phi) = ae^\phi$  evades Bekenstein’s theorem, a result which opened the way to find new black-hole solutions, the so-called dilatonic black holes. In the context of the present analysis, it is clear that the exact form of the coupling function is again of no importance. Thus, we set off looking for new black holes in the context of the theory (7) choosing various forms for  $f(\phi)$ . For each form, we numerically integrated the system of equations (12), by giving the input values  $(\phi_h, \phi'_h)$ . The first quantity was a free parameter constrained only by the condition (15) while the second one was uniquely determined by the regularity constraint (14) of the black-hole horizon. Using this method, every pair of initial values  $(\phi_h, \phi'_h)$  leads to a regular black-hole solution with a non-trivial scalar hair. In this way, we determined a large number of black-hole solutions with scalar hair for a variety of forms of the coupling function  $f(\phi)$ : exponential, odd and even power-law, odd and even inverse-power-law. An indicative subset of solutions for the scalar field are depicted in the left plot of Fig. 1 while, on the right plot, we present the profile of the two metric functions (in absolute value) with the characteristic form of an asymptotically-flat black-hole geometry. We should note at this point that our analysis covers both the case of *spontaneous scalarisation* (i.e. the case where the Schwarzschild solution arises as an independent solution) and the case of *natural scalarisation* (where the Schwarzschild solution does not emerge) depending on the particular choice of the coupling function  $f(\phi)$ .

In Fig. 2, we present some of the properties of the scalarised black holes for the indicative case of  $f(\phi) = a/\phi$ . The left plot presents the scalar charge  $D$ , that characterises the scalar field at infinity. As is clear, this quantity is in fact a

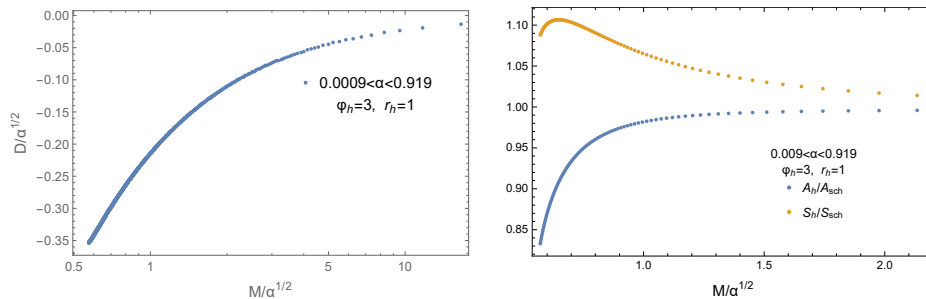


**Fig. 2.** The scalar charge  $D$  (left plot), and the ratios  $A_h/A_{Sch}$  and  $S_h/S_{Sch}$  (right plot, lower and upper curve respectively) in terms of the mass  $M$ , for  $f(\phi) = a/\phi$  [55].

function of the black-hole mass, a result that renders the scalar hair secondary. Also, a common characteristic in all cases is that, as the mass of the black hole increases, the scalar charge decreases and eventually vanishes as our black-hole solution matches the Schwarzschild solution. In other words, every massive GB scalarised black hole reduces to the Schwarzschild solution.

The right plot of Fig. 2 depicts two important quantities, the horizon area of the black hole, given by  $A_h = 4\pi r_h^2$  and normalised in units of the horizon area of the Schwarzschild solution with the same mass, and the entropy of the black hole normalised again in units of the entropy of the corresponding Schwarzschild solution. Starting from the horizon area, we observe that this ratio is always smaller than unity, which means that all GB black-hole solutions are smaller than their GR analogues. This is due to the effect of the GB term which exerts a positive (outward) pressure and which can be counterbalanced only by “squeezing” further the available energy/mass distribution thus resulting into smaller black holes. We also observe that the area curve stops abruptly at its lower end, thus exhibiting the existence of a lower bound on the horizon area and thus on the mass of the black hole. Beyond this lower value, the black hole ceases to exist — this feature is due to the bound (15) discussed earlier. The entropy of the black-hole solutions may be computed, for an arbitrary form of  $f(\phi)$ , following various methods [36][56], and it is found to be

$$S_h = \frac{A_h}{4} + 4\pi f(\phi_h). \quad (23)$$

The profile of the entropy  $S_h$  of a GB black hole compared to the one of the Schwarzschild black hole,  $S_{Sch} = A_h/4$ , depends strongly on the choice for the particular form of the coupling function. For instance, for the choice employed in this case, i.e. the inverse linear form, the entropy ratio comes out to be larger than unity for the entire mass range, a result that renders this particular family of solutions more thermodynamically stable than the corresponding Schwarzschild black hole. For different forms of the coupling function though, the curve of the entropy ratio may lie in whole or in parts below unity thus revealing an instability for the entire or parts of the mass regime. In all cases, as the mass  $M$

increases, the entropy ratio always reduces to unity as the Schwarzschild limit is approached.

The theory (7) allows not only asymptotically-flat black-hole solutions but also black holes with an asymptotically Anti-de Sitter behaviour. This follows if we add to the theory a cosmological constant bringing the action functional of the theory to the form [58]

$$S = \frac{1}{16\pi} \int d^4x \sqrt{-g} \left[ R - \frac{1}{2} \partial_\mu \phi \partial^\mu \phi + f(\phi) R_{GB}^2 - 2\Lambda \right]. \quad (24)$$

In this case, the field equations (10) remain unchanged apart from the shift

$$T_{\mu\nu} \rightarrow T_{\mu\nu} - \Lambda g_{\mu\nu}. \quad (25)$$

Apart from the change in the spacetime background at large distances, we expect that the profile of the scalar field will also be affected. Indeed, imposing as before the regularity of its second derivative  $\phi''$  at the black-hole horizon, the field equations lead to the modified constraint

$$\phi'_h = \frac{16Ar_h \dot{f}^2 (Ar_h^2 - 3) + Ar_h^5 - r_h^3 \mp \sqrt{C}}{4\dot{f}[r_h^2 - \Lambda(r_h^4 - \dot{f}^2)]}, \quad (26)$$

where all quantities have been evaluated at  $r_h$ . The quantity  $C$  under the square root stands for the following combination

$$C = 256\Lambda \dot{f}_h^4 (Ar_h^2 - 6) + 32r_h^2 \dot{f}_h^2 (2Ar_h^2 - 3) + r_h^6 \geq 0, \quad (27)$$

and must always be non-negative for  $\phi'_h$  to be real. Under the validity of the constraint (26), the asymptotic form of the solution for the metric function and the scalar field takes the same functional form as the one given in (17).

Assuming the presence of a negative cosmological constant, and expecting the spacetime to assume a form close to that of the Schwarzschild-Anti-de Sitter solution at large distances, we find that the approximate forms for the metric functions in that regime is

$$e^{A(r)} = \left( k - \frac{2M}{r} - \frac{\Lambda_{eff}}{3} r^2 + \frac{q_2}{r^2} \right) \left( 1 + \frac{q_1}{r^2} \right)^2, \quad (28)$$

$$e^{-B(r)} = k - \frac{2M}{r} - \frac{\Lambda_{eff}}{3} r^2 + \frac{q_2}{r^2}, \quad (29)$$

where  $k$ ,  $M$ ,  $\Lambda_{eff}$  and  $q_{1,2}$  are arbitrary constants. Regarding the asymptotic form of the scalar field, this is given by

$$\phi(r) = \phi_\infty + d_1 \ln r + \frac{d_2}{r^2} + \frac{d_3}{r^3} + \dots, \quad (30)$$

where again  $(\phi_\infty, d_1, d_2, d_3)$  are arbitrary constant coefficients. In principle, the scalar field assumes this form in the case of a linear coupling function,  $f(\phi) = a\phi$

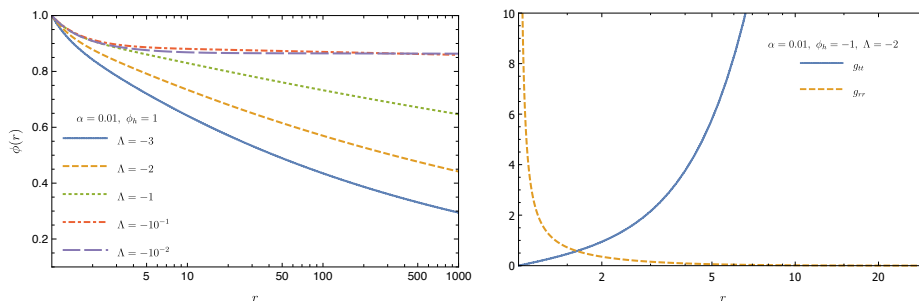


**Fig. 3.** The solution for the scalar field  $\phi$  (left plot), and for the metric components  $|g_{tt}|$  and  $g_{rr}$  (right plot) in terms of the radial coordinate  $r$ , for  $f(\phi) = a\phi^2$  [56].

[59][60], however, it may be shown numerically that it holds in the perturbative limit of small GB coupling constant  $a$ , for all forms of the coupling function. We notice that the dominant term in the expression of  $\phi$  at large distances has a logarithmic form and not an  $1/r$  dependence; as a result, no scalar charge may be attributed to any scalarised solution found. In contrast, the coefficient  $M$  in the asymptotic form of the metric functions may be interpreted again as the gravitational mass of the solution.

As in the case of zero cosmological constant, a plethora of solutions emerged from the numerical integration of the set of field equations under the appropriate boundary conditions. Ensuring that the input quantity  $\phi'_h$  is given by the expression (26), black-hole solutions with an asymptotically Anti-de Sitter behaviour emerged for all different choices of the coupling function, namely  $f(\phi) = e^{\pm\phi}$ ,  $\phi^{\pm 2n}$ ,  $\phi^{\pm(2n+1)}$ ,  $\ln \phi$ , ... [58]. The profiles of both the scalar field and the metric functions are given in the left and right plot, respectively, of Fig. 3.

We may finally promote the negative cosmological constant to a dynamic potential for the scalar field [61] as follows

$$S = \int d^4x \sqrt{-g} \left[ \frac{R}{16\pi G} - \frac{1}{2} \partial_\mu \phi \partial^\mu \phi + f(\phi) R_{GB}^2 - 2\Lambda V(\phi) \right]. \quad (31)$$

We will insist again on the case of the negative coupling constant, i.e.  $\Lambda < 0$ , and consider different choices for the coupling function  $f(\phi)$  and the scalar potential  $V(\phi)$ . Demanding again the regularity of the black-hole horizon and repeating the aforementioned analysis, we may determine a similar constraint on the value of  $\phi'_h$ . This quantity may be used again as an input parameter, together with  $\phi_h$ , for the numerical integration of the field equations, once a specific form for  $f(\phi)$  and  $V(\phi)$  is chosen. Again, for every possible choice of these two scalar functions, black-hole solutions with a regular horizon and a non-trivial  $\phi$  emerged.

In Fig. 4 (left plot), we present the profile of the scalar field in terms of the radial coordinate for many different (polynomial) choices of the scalar potential, and for fixed form of the coupling function, i.e.  $f(\phi) = ae^\phi$ . We observe that for  $\Lambda < 0$ , the scalar field oscillates around the zero value where it finally relaxes.

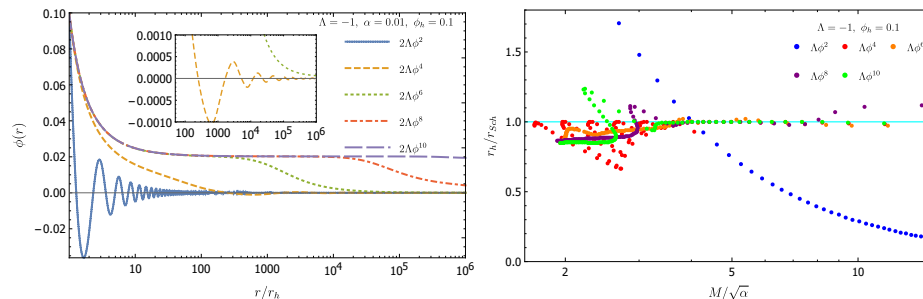


**Fig. 4.** The profile of the scalar field in terms of the radial coordinate for different (polynomial) choices of the scalar potential (left plot); the lines of existence of the black-hole solutions for the same choices of  $V(\phi)$  (right plot) [61].

As the degree of the polynomial increases, the relaxation time gets longer. In the right plot, we depict the domain of existence of the black-hole solutions under the same choices. Here, we notice a different pattern for the solutions emerging for  $V(\phi) = \Lambda\phi^2$  from the one assumed for the other polynomial forms. In the latter cases, the black-hole solutions form branches which are more prominent in the small-mass regime but tend to smooth out and eventually match the horizon value of the corresponding Schwarzschild solution. In the case of a quadratic scalar potential, the solutions present a distinctly different pattern: the solutions form a monotonically decreasing line of existence spanning the whole regime, from large- $r_h$ , low-mass black holes to small- $r_h$ , large-mass black holes. The theory therefore includes *ultra-sparse* black holes, *Schwarzschild-like* black holes and *ultra-compact* black holes. The study of the entropy reveals a similar behaviour in terms of the mass as the horizon radius; as a result, the ultra-sparse black holes are found to be more thermodynamically stable compared to the Schwarzschild-like black holes, and these in turn to be more thermodynamically stable compared to the ultra-compact black holes.

The discussion above summarizes only a small part of the black-hole solutions that have been found in the context of gravitational theories containing the GB or related terms. There is in fact a huge literature in this topic and the interested reader may find more results in [62]-[151].

### 3.2 Wormholes in Einstein-Scalar-GB Theory

As we stated in Section 2, General Relativity does not accommodate *traversable* wormholes. We also claimed that the Ellis-Bronnikov solution, which emerges in the context of the Einstein-scalar theory, is supported in fact by a ghost scalar field. Is there a particular feature of the wormhole geometry that makes it incompatible with GR or simple extensions of it? Actually, there is.

To demonstrate this, we will employ the Morris-Thorne method for the construction of wormhole solutions [21]. This method also incorporates the alternative approach mentioned in Section 2, in which traversable wormhole solutions

may emerge only in the absence of a horizon or singularity. According to the analysis of [21], a traversable wormhole may be described by the following line-element

$$ds^2 = -e^{2\Phi(r)} dt^2 + \left(1 - \frac{b(r)}{r}\right)^{-1} dr^2 + r^2 (d\theta^2 + \sin^2 \theta d\varphi^2). \quad (32)$$

The *red-shift* function  $\Phi$  must be everywhere finite. The *shape* function  $b$  must satisfy  $1 - b/r \geq 0$  throughout spacetime, and is allowed to vanish at a single point, i.e. at  $r = b = b_0$ , where the throat of the wormhole is located. At infinity,  $\Phi$  and  $b/r$  must both vanish to recover the asymptotically flat regime.

To study the geometric structure of the above solution, we construct its embedding diagram. To this end, we equate the line-element of the 2D spacelike equatorial surface, obtained for  $t = \text{const.}$  and  $\theta = \pi/2$ , with the one of a 3D Euclidean space:

$$\frac{dr^2}{1 - b/r} + r^2 d\varphi^2 \equiv dz^2 + d\rho^2 + \rho^2 d\varphi^2 = \left[ \left(\frac{dz}{d\rho}\right)^2 + 1 \right] d\rho^2 + \rho^2 d\varphi^2. \quad (33)$$

From the above, we obtain immediately that  $\rho = r$ . We demand that both line-elements describe the same geometry and equate the coefficients of  $dr^2$  in (33). Then, the “fictitious”  $z$  coordinate is given by the relation

$$\frac{dz}{dr} = \pm \left(\frac{r}{b} - 1\right)^{-1/2} \Rightarrow z(r) = \pm \int_{b_0}^r \left(\frac{r}{b} - 1\right)^{-1/2} dr, \quad (34)$$

and describes the lift of the  $(r, \varphi)$ -plane due to the curvature of spacetime. At infinity, as  $b/r \rightarrow 0$ , we obtain  $dz/dr \rightarrow 0$ , and the embedding surface becomes parallel to the  $(r, \varphi)$ -plane exhibiting no lift due to the flatness of this regime. In contrast, near the throat, the slope diverges and this signifies that the embedding surface at this point is vertical. Therefore,  $\{\rho(r), z(r)\}$  is a parametric representation of a slice of the embedded  $\theta = \pi/2$ -plane for a fixed value of the  $\varphi$  coordinate, while the corresponding surface of revolution is the 3-D representation of the wormhole’s geometry. The typical embedding diagram of a wormhole is given in Fig. 5.

One could invert the function  $z(r)$  to obtain  $r(z)$ . Then, from Fig. 5, it is clear that  $r(z)$  possesses a minimum at the throat and then “flares outwards” as we approach the asymptotically flat region. Therefore, the existence of a throat is mathematically ensured if the following two conditions hold

$$\left. \frac{dr}{dz} \right|_{r_0} = 0, \quad \left. \frac{d^2 r}{dz^2} \right|_{r_0} > 0. \quad (35)$$

The first condition is satisfied since, as we showed above,  $dz/dr \rightarrow 0$  at  $r = r_0$ . The second condition takes the form

$$\frac{d^2 r}{dz^2} = \frac{b - rb'}{2b^2} > 0, \quad (36)$$

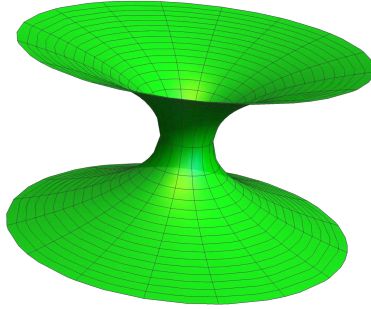


**Fig. 5.** The embedding diagram of a typical traversable wormhole.

and is known as the *flaring-out* condition of the wormhole. Therefore, in order to have a throat, the shape function  $b(r)$  should satisfy  $b - rb' > 0$ , which fully justifies its name.

In fact, the flaring-out condition leads to the violation of energy conditions in a wormhole background since it imposes a certain behaviour on the shape function and, through Einstein's equations, on the matter content of the theory. Let us focus on the Null Energy Condition (NEC) which has the form:

$$T_{\mu\nu}n^\mu n^\nu = -g_{tt}(T_r^r - T_t^t) = -g_{tt}(\rho + p_r) \geq 0, \quad (37)$$

where  $T_{\mu\nu}$  is the energy-momentum tensor and  $n^\mu$  any null vector satisfying  $n^\mu n_\mu = 0$ . For  $g_{tt} < 0$ , the above demands that  $\rho + p_r \geq 0$ . However, through Einstein's equations and using the line-element (32), we obtain

$$8\pi G(\rho + p_r) = G_r^r - G_t^t = -\frac{(b - rb')}{r^3} \Big|_{r=r_0} < 0, \quad (38)$$

where we used the flaring-out condition (36). As a result, the wormhole geometry may be supported by some distribution of matter which violates the energy conditions and instead satisfies the condition  $\rho + p_r < 0$ . That is why pure GR cannot support a traversable wormhole nor can the Einstein-scalar theory with a physical scalar field do it either.

It becomes therefore clear that a more involved gravitational theory beyond GR is necessary in order to support viable wormhole solutions. Can we find such a physical theory? The Einstein-scalar-GB theory is a theory which violates the energy conditions, as the evasion of no-hair theorems clearly demonstrated. However, this violation is not caused by the introduction of some form of exotic matter but by the direct coupling of a physical scalar field to the quadratic, gravitational GB term. Can this violation then support wormhole solutions?

In [28], where the dilatonic black holes were first discovered, in the context of the EsGB theory with an exponential coupling function,  $f(\phi) = a e^\phi$ , another



class of solutions were presented with the line-element having the form of a Morris-Thorne solution. By applying a coordinate transformation [152][153], this was written as

$$ds^2 = -e^{A(\ell)} dt^2 + e^{B(\ell)} d\ell^2 + (\ell^2 + r_0^2) (d\theta^2 + \sin^2 \theta d\varphi^2), \quad (39)$$

where  $\ell$  is a new spacelike coordinate ranging in the interval  $(-\infty, \infty)$ . The above line-element describes a wormhole connecting two asymptotically-flat regimes and with a radius throat  $r_0$  at  $\ell = 0$ . In this new coordinate system, both metric functions and the scalar field assume regular forms in the regime close to the throat, namely

$$e^{A(\ell)} = a_0 + a_1 \ell + \dots, \quad e^{B(\ell)} = b_0 + b_1 \ell + \dots, \quad \phi(\ell) = \phi_0 + \phi_1 \ell + \dots \quad (40)$$

On the other hand, at large distances, we obtain power-law expansions in terms of  $(1/r)$

$$e^A \simeq 1 - \frac{2M}{\ell} + \dots, \quad e^B = 1 + \frac{2M}{\ell} + \dots, \quad \phi \simeq \phi_\infty + \frac{D}{\ell} + \dots, \quad (41)$$

where  $M$  and  $D$  are the mass and scalar charge of the wormhole. Note that these expansions are identical to the ones for a black-hole solution with the exception that here  $M$  and  $D$  are independent quantities.

Employing these asymptotic solutions as boundary conditions, the set of field equations (10) were numerically solved again, this time in quest of wormhole solutions [152][153]. And such solutions were indeed found, with the spacetime background having the geometry depicted in Fig. 5 and the scalar field assuming the profile presented on the upper plot of Fig. 6. However, a true singularity was lurking behind the throat, at the negative  $\ell$  regime. Thus, a traversable, symmetric solution was built by cutting the spacetime at  $\ell = 0$  and gluing the positive regular  $\ell$ -regime with its mirror image along  $\ell < 0$ . At the gluing point  $\ell = 0$ , cusps were created whose presence could be justified only by introducing a distribution of a (non-exotic!) perfect fluid and a gravitational source term around the throat. This distribution is described by the action functional [152][153]

$$S_3 = \int d^3x \sqrt{h} (\lambda_1 + \lambda_0 e^\phi \tilde{R}), \quad (42)$$

where  $(\lambda_1, \lambda_2)$  are constants and  $\tilde{R}$  is the scalar curvature of the 3-dimensional induced spacetime at  $\ell = 0$ . Under the above construction, a regular wormhole solution is constructed which can be traversed both by null and timelike particles. A set of particle trajectories, which start from one asymptotically-flat regime, traverse the throat, reach the asymptotically-flat regime on the other side of the wormhole and then travel back to the starting point, are presented on the lower plot of Fig. 6.

All the above results were derived in the context of the dilatonic Einstein-scalar-GB theory, that is with an exponential coupling function. Can we generalise this analysis and produce similar wormhole solutions in the context of

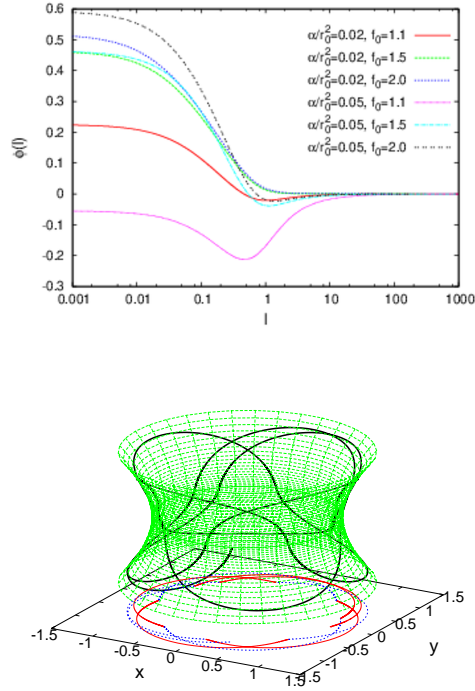


**Fig. 6.** The solutions for the scalar field for a family of dilatonic wormholes (upper plot), and particles trajectories in the background of a dilatonic wormhole (lower plot) [152][153].

the EsGB theory with alternative forms for  $f(\phi)$ , as in the case of black holes? In the context of the general theory (7), we looked indeed for viable wormhole solutions following a similar approach as above. Apart from the form of the coupling function, we incorporated also a different form of line-element, namely the following [154]

$$ds^2 = -e^{A(\eta)} dt^2 + e^{\Gamma(\eta)} [d\eta^2 + (\eta^2 + \eta_0^2) (d\theta^2 + \sin^2 \theta d\varphi^2)]. \quad (43)$$

This new ansatz modifies the conditions for the existence of a sole minimum in the function  $r(z)$  in the embedding diagram, and allows for multiple extremal points and thus for a much richer topology: local maxima correspond to the so-called *equators* whereas local minima give rise to *multiple throats*.

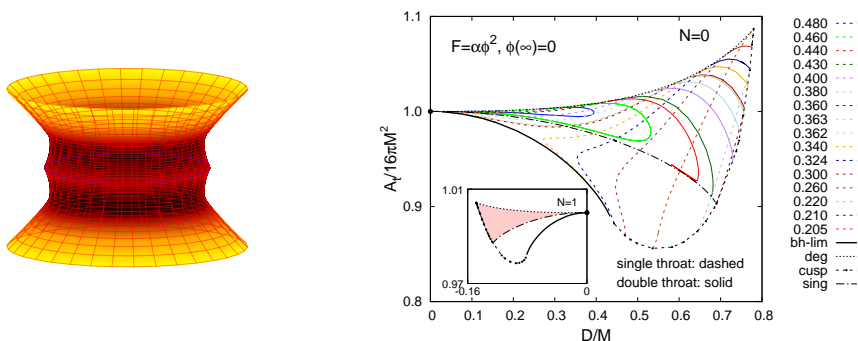


**Fig. 7.** A wormhole solution with an equator and two throats (left plot), and the domain of existence of wormhole solutions in the case where  $f(\phi) = a\phi^2$  (right plot) [154].

The metric functions and scalar field assume regular forms both near the throat and the far asymptotic regime. The numerical integration yielded a large number of wormhole solutions, for every form of  $f(\phi)$  used, with an asymptotically-flat behaviour and with a single throat or with a double throat and an equator. The embedding diagram of a wormhole in the latter case is shown on the left plot of Fig. 7. All solutions were made traversable by employing the same cut & paste technique, where the spacetime with  $\ell > 0$  was glued at  $\ell = 0$  with its mirror image along  $\ell < 0$ . As before, a distribution of regular matter around the throat suffices to justify the cusps at the gluing point. On the right plot of Fig. 7, we present the domain of existence of wormhole solutions in the indicative case of quadratic coupling function,  $f(\phi) = a\phi^2$ . All EsGB wormhole solutions are bounded by the corresponding black-hole solutions which form the left boundary of the domain.

For additional works on wormhole solutions arising in the context of generalised gravitational theories involving scalar fields or higher-curvature terms see, for instance, [155]-[165].

### 3.3 Particle-like Solutions in Einstein-Scalar-GB Theory

Let us finally address the last class of compact objects, the gravitational particle-like solutions. As was mentioned, in the context of the minimal Einstein-scalar theory, the corresponding Fisher/Janis-Newman-Winicour-Wyman particle-like solution [24] is irregular. Can we hope to find particle-like solutions which however behave better in the context of the EsGB theory?

With this in mind, we looked for static, spherically-symmetric solutions which describe a regular spacetime, with no singularities or horizons and no throats as well [166][167]. We chose to work with the following form of line-element

$$ds^2 = -e^{A(r)} dt^2 + e^{\Gamma(r)} [dr^2 + r^2 (d\theta^2 + \sin^2 \theta d\varphi^2)], \quad (44)$$

with two unknown metric functions,  $A(r)$  and  $\Gamma(r)$ , as usual. The above form was inspired by the one employed in our quest for wormhole solutions and resulted, as we saw, in a much richer topology of these solutions around the throat. Here, we will use a similar line-element in the hope that solutions with features not allowed or often observed, when more restrictive ansatzes are used, will now emerge.

The set of field equations of the theory (10) must now be solved for the three unknown functions, the two metric functions and the scalar field  $\phi(r)$ . If we substitute the above ansatz for the line-element in the field equations, we obtain four, coupled, ordinary differential equations which can further be reduced to a system of only two independent equations for  $A(r)$  and  $\phi(r)$ . The remaining metric function  $\Gamma(r)$  can be determined once the solutions for  $A(r)$  and  $\phi(r)$  are found.

The set of the two independent, second-order differential equations was solved numerically under the proper boundary conditions. We demanded a regular form for both functions over the entire radial regime, an asymptotically-flat behaviour at large distances and a smooth solution close to the origin. At large distances, we obtained indeed an asymptotically-flat behaviour, which was identical to the one for black holes and wormholes, namely

$$e^{A(r)} \simeq 1 - \frac{2M}{r} + \dots, \quad \phi \simeq \phi_\infty - \frac{D}{\ell} + \dots, \quad (45)$$

where  $M$  and  $D$  are once again the mass and the scalar charge of the solution. The expansion near the origin of the radial coordinate was found to be more involved and to depend on the form of the coupling function  $f(\phi)$ . For instance, for a quadratic form,  $f(\phi) = \alpha\phi^2$ , we find the asymptotic solution

$$A(r) = A_0 + A_2 r^2 + A_3 r^3 + \dots, \quad (46)$$

$$\phi = -\frac{c_0}{r} + \phi_0 + \phi_1 r + \phi_2 r^2 + \phi_3 r^3 + \dots. \quad (47)$$

We readily observe that the metric is indeed regular near the origin but the scalar-field expansion features a singular term with a divergent behaviour at small  $r$ . In fact, the presence of this term seems to be a generic feature of the expansion of the scalar field near the origin independently of the form of the coupling function. The numerical integration of the system of field equations led to the complete solution which, as expected, interpolated between the two asymptotic forms. The profile of the complete solutions for the metric and scalar field are depicted, for the quadratic coupling function, on the left plot of Fig. 8 [166][167].

In order to investigate the consequences of the singular term, present in the expansion of the scalar field near the origin, we computed all gravitational scalar invariants as well as the components of the energy-momentum tensor  $T_{\mu\nu}$ . Despite the singularity in  $\phi$ , all these quantities were found to be finite over the entire radial regime. The exact values of the energy-density and pressure at the

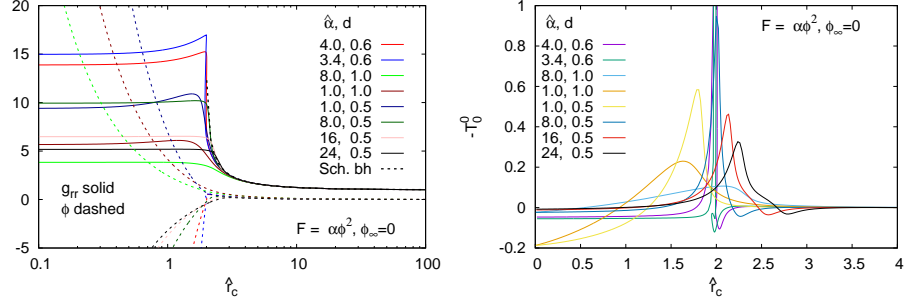


**Fig. 8.** The solutions for the metric and scalar field (left plot) and the corresponding energy-density (right plot) in the case of the quadratic coupling function [166][167].

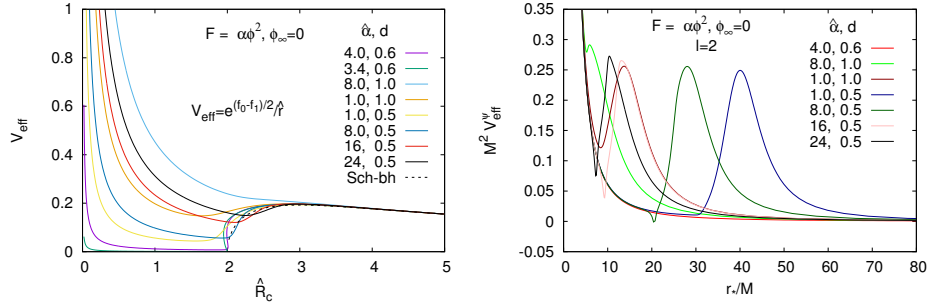


**Fig. 9.** The effective potential for null particles (left plot) and for test scalar particles (right plot), for a quadratic coupling function [166][167].

origin are given below:

$$\rho(0) = -\frac{3}{32\alpha}, \quad p(0) = \frac{2}{32\alpha}. \quad (48)$$

We may therefore conclude that the singularity of the scalar field at the origin has no physical consequence, and that the situation resembles more the behaviour of the Coulomb potential which also diverges at the origin of the coordinate system.

The complete profile of the energy-density  $\rho$  of an indicative particle-like solution is depicted on the right plot of Fig. 8. We observe that it has a regular, shell-like behaviour, and vanishes quickly at a very small distance from the origin. We may therefore conclude that our gravitational particle-like solutions are more *bubble-shaped* than point-like, and clearly qualify as *ultra-compact* objects (see also [168]-[171]).

The propagation of test particles in the background of the aforementioned gravitational bubble-shaped solutions may lead to interesting observable phenomena. The geodesics for both null and timelike particles may be found from

their Lagrangian  $\mathcal{L}$  given by the expression

$$2\mathcal{L} = g_{\mu\nu}\dot{x}^\mu\dot{x}^\nu = -e^{f_0}\dot{t}^2 + e^{f_1}\left[\dot{r}^2 + r^2\left(\dot{\theta}^2 + \sin^2\theta\dot{\varphi}^2\right)\right] = -\epsilon, \quad (49)$$

where  $\epsilon = 0$  and  $1$  for massless and massive particles, respectively. Employing the two conserved quantities, namely the energy  $E = -e^{f_0}\dot{t}$  and the angular-momentum  $L = e^{f_1}r^2\dot{\varphi}$  of the particle, and considering motion in the equatorial plane ( $\theta = \pi/2$ ), we obtain the following equation for null particles

$$e^{f_0+f_1}\dot{r}^2 = (E + LV_{\text{eff}})(E - LV_{\text{eff}}), \quad (50)$$

where  $V_{\text{eff}} = e^{(f_0-f_1)/2}/r$  is the effective potential for photons. We depict its form in terms of the scaled circumferential coordinate  $\hat{R}_c = e^{f/2}r$  in Fig. 9, for the coupling function  $F = \alpha\phi^2$ . Whereas, for the less compact particle-like solutions, the effective potential is monotonic, for the more compact solutions, the effective potential  $V_{\text{eff}}$  is characterised by a pair of extrema. These extrema correspond to circular orbits and thus lead to the presence of *light rings* around these ultra-compact solutions. Bound orbits emerge also for massive particles with radii smaller than or comparable to the radius of the bubble. In fact, it is found that particles may pass over the origin ( $r = 0$ ) or even rest there without encountering any divergence from the singular term in the expression of the scalar field.

We also considered the propagation of a scalar test particle  $\Psi$  in this background. Starting from the equation  $\square\Psi = 0$  and expanding the scalar field in spherical harmonics  $Y_l^m(\theta, \varphi)$ ,

$$\Psi(t, r, \theta, \varphi) = \sum_{l,m} \psi_{l,m}(t, r) e^{-f_1/2} Y_l^m(\theta, \varphi) / r, \quad (51)$$

we obtain the reduced equation

$$(\partial_t^2 - \partial_{r_*}^2 + V_{\text{eff}}^\psi) \psi_{l,m}(t, r) = 0, \quad (52)$$

where  $r_*$  is the tortoise coordinate defined through the relation  $dr_* = e^{(f_1-f_0)/2}dr$ , and  $V_{\text{eff}}^\psi$  is the scalar-field effective potential

$$V_{\text{eff}}^\psi = e^{f_0-f_1} \left[ \frac{l(l+1)}{r^2} + \frac{2(f_1' + f_0') + r f_1' f_0' + 2r f_1''}{4r} \right]. \quad (53)$$

The form of the scaled effective potential  $M^2 V_{\text{eff}}^\psi$  versus the scaled tortoise coordinate  $r_*/M$  is presented on the right plot of Fig. 9, again for a quadratic coupling function. We observe that, for scalar waves with  $l > 0$ , the effective potential features an infinite barrier that resides at the origin and a finite local barrier at a larger value of  $r_*$ . An incoming scalar-wave with  $l > 0$  will be partially transmitted through the finite local barrier and will then undergo a perpetual process of full and partial reflection from the infinite and finite barrier, respectively, thus producing a series of *echoes* in the wave signal.

## 4 Compact Objects in (beyond) Horndeski Theory

The Einstein-scalar-GB theory is a special case of a more general tensor-scalar theory of a single scalar degree of freedom with field equations containing only up to 2nd-order derivatives, the *Horndeski theory* [11]. The latter is defined through the Lagrangian

$$S_H = \int d^4x \sqrt{-g} (\mathcal{L}_2 + \mathcal{L}_3 + \mathcal{L}_4 + \mathcal{L}_5)$$

with

$$\begin{aligned} \mathcal{L}_2 &= G_2(X), & \mathcal{L}_3 &= -G_3(X) \square \phi, \\ \mathcal{L}_4 &= G_4(X)R + G_{4X} [(\square \phi)^2 - \nabla_\mu \partial_\nu \phi \nabla^\mu \partial^\nu \phi], \\ \mathcal{L}_5 &= G_5(X)G_{\mu\nu} \nabla^\mu \partial^\nu \phi - \frac{1}{6} G_{5X} [(\square \phi)^3 - 3 \square \phi \nabla_\mu \partial_\nu \phi \nabla^\mu \partial^\nu \phi \\ &\quad + 2 \nabla_\mu \partial_\nu \phi \nabla^\nu \partial^\rho \phi \nabla_\rho \partial^\mu \phi]. \end{aligned}$$

The coupling functions  $G_i$  depend on the scalar field  $\phi$  only through its kinetic term  $X \equiv -\nabla_\mu \phi \nabla^\mu \phi / 2$ , thus the above theory is the special, *shift-symmetric* Horndeski theory. The symbol  $G_{iX}$  above denotes the derivative of the function  $G_i$  with respect to  $X$ .

Although the theory is more complicated compared to the Einstein-scalar-Gauss-Bonnet theory and the determination of analytic solutions therefore seems unlikely, in fact the presence of all the additional terms and the freedom we have in choosing the exact form of the coupling functions  $G_i$  of the theory can help in deriving new analytic solutions. Indeed, whereas this possibility does not exist in the context of the EsGB theory, a wise choice for the form of  $G_i$  in Horndeski theory can turn the set of field equations into an integrable set of equations, which can then be solved analytically. For instance, choosing the following coupling functions

$$G_2 = 8\alpha X^2, \quad G_3 = -8\alpha X, \quad G_4 = 1 + 4\alpha X, \quad G_5 = -4\alpha \ln |X|, \quad (54)$$

a static, spherically symmetric black-hole solution of the form

$$ds^2 = -h(r) dt^2 + \frac{dr^2}{f(r)} + r^2 d\Omega^2, \quad (55)$$

with  $h(r) = f(r)$ , was analytically derived in the context of the Horndeski theory with the metric function and scalar field having the following explicit forms [172][173]

$$h(r) = 1 + \frac{r^2}{2\alpha} \left( 1 - \sqrt{1 + \frac{8\alpha M}{r^3}} \right), \quad \phi' = \frac{\sqrt{h} - 1}{r\sqrt{h}}, \quad (56)$$

respectively. The above solution describes an asymptotically-flat black hole with a non-trivial scalar field and a horizon at  $r_H = M + \sqrt{M^2 - \alpha}$ , where  $M$  is the black-hole mass and  $\alpha$  the coupling constant of the theory.

The Horndeski theory is certainly not the end of the road when it comes to generalised tensor-scalar theories. One could extend this theory to *beyond Horndeski* by adding the following well-known terms

$$\mathcal{L}_4^{\text{bH}} = F_4(X)\varepsilon^{\mu\nu\rho\sigma}\varepsilon^{\alpha\beta\gamma}{}_{\sigma}\partial_{\mu}\phi\partial_{\alpha}\phi\nabla_{\nu}\partial_{\beta}\phi\nabla_{\rho}\partial_{\gamma}\phi \quad (57)$$

$$\mathcal{L}_5^{\text{bH}} = F_5(X)\varepsilon^{\mu\nu\rho\sigma}\varepsilon^{\alpha\beta\gamma\delta}\partial_{\mu}\phi\partial_{\alpha}\phi\nabla_{\nu}\partial_{\beta}\phi\nabla_{\rho}\partial_{\gamma}\phi\nabla_{\sigma}\partial_{\delta}\phi. \quad (58)$$

Despite the presence of the above terms, the theory remains free of ghosts provided that the coupling functions  $(G_4, G_5)$  and  $(F_4, F_5)$  of the extended theory satisfy the constraint [174]

$$XG_{5X}F_4 = 3F_5(G_4 - 2XG_{4X}). \quad (59)$$

In the context of the beyond Horndeski theory, the complexity of the field equations increases further, and the integrability of the system of equations is easily lost. However, by employing a number of auxiliary functions, we managed to bring the complicated equations of motion to a very simple form, namely [175]

$$\begin{aligned} X'\mathcal{A} &= 2\left(\frac{h'}{h} - \frac{f'}{f}\right)\mathcal{B}, \\ \frac{h'f}{2h}\mathcal{A} &= G_{2X}r^2 + 2G_{4X} - 2rf\phi'G_{3X} - 2fZ_X, \\ 2f\frac{h'}{h}\mathcal{B} &= -G_2r^2 - 2G_4 - 2fZ, \end{aligned} \quad (60)$$

where  $\mathcal{A}$ ,  $\mathcal{B}$  and  $Z$  are functions of  $\{G_i, F_i, X\}$  given by the expressions

$$\begin{aligned} \mathcal{A} &= 4rZ_X + \phi' [r^2G_{3X} + G_{5X}(1 - 3f) - 2XfG_{5XX} + 12fX(5F_5 + 2XF_{5X})], \\ \mathcal{B} &= rZ - f\phi'XG_{5X} + 12f\phi'X^2F_5, \\ Z &= 2XG_{4X} - G_4 + 4X^2F_4, \end{aligned} \quad (61)$$

and  $(h, f)$  are the two metric functions of the static, spherically-symmetric line-element (55).

In the context of the parity-symmetric theory, i.e. with  $G_3 = G_5 = F_5 = 0$ , the above set of field equations is easily rendered integrable and may lead to a large number of analytic solutions. For instance, for the general class of theories where

$$G_2 = -2\Lambda - \alpha X + \delta X^m, \quad G_4 = \zeta + \beta X^n, \quad (62)$$

where  $(\Lambda, \alpha, \delta, \zeta, \beta)$  are constant parameters of the theory and  $(m, n)$  real, integer or rational numbers, and  $Z$  chosen to be a constant, a large number of analytical homogeneous solutions with  $f(r) = h(r)$  were derived [175]. These solutions were characterized at the small- $r$  regime by zero, one or two horizons, depending on the values of the parameters of the theory, while at large distances they assumed an (Anti-)de Sitter-Reissner-Nordstrom-type of behaviour of the form

$$h(r) = 1 - \frac{\Lambda_{eff}r^2}{3} - \frac{2M}{r} + \frac{Q^2}{r^2}. \quad (63)$$



In the expression above,  $M$  is the ADM mass of the solution,  $\Lambda_{eff}$  the effective cosmological constant and  $Q$  a tidal charge. The first parameter is an arbitrary integration constant while the latter two are determined by the coupling parameters of the theory. All solutions are characterized by a non-trivial scalar field, which at large distances behaves as  $\phi' \sim 1/h(r)$  while it diverges at the (outer) horizon, when the latter exists; however,  $X$  remains everywhere finite as also does the energy-momentum tensor of the theory. By making appropriate, alternative choices for the coupling functions of the theory, non-homogeneous solutions, with  $f \neq h$  but with the same asymptotic behaviour, were also found.

In the case of no parity symmetry, when the functions  $(G_3, G_5, F_5)$  in principle do not vanish, the set of equations becomes significantly more difficult to solve. Nevertheless, even in this case, our formalism allows for the integration of this set, under convenient choices for the coupling and auxiliary functions of the theory, and new black-hole solutions, which generalise the solution of [172], can be determined, albeit in a non-explicit form over the entire radial regime [175]. Additional black-hole solutions determined in the context of Horndeski or beyond Horndeski theory can be found in [176]-[178].

In the context of beyond Horndeski theory, wormhole solutions may also be found. However, instead of solving the set of field equations for the desired type of solution, one could follow an alternative technique [179] [180] and apply an appropriate *disformal transformation* [181][182][183] to a known solution denoted by  $(\bar{g}_{\mu\nu}, \bar{\phi})$ . A disformal transformation has the general form

$$g_{\mu\nu} = \bar{g}_{\mu\nu} - D(\bar{X}) \nabla_\mu \bar{\phi} \nabla_\nu \bar{\phi}, \quad \phi = \bar{\phi}, \quad (64)$$

where  $D(X)$  is an arbitrary function which characterizes the disformal transformation. According to the above, the components of the metric tensor get transformed in a way that depends on the configuration of the scalar field while the latter remains unchanged. In this way, one could start from a known solution  $(\bar{g}_{\mu\nu}, \bar{\phi})$  and obtain a new one  $(g_{\mu\nu}, \phi)$ . When the “seed solution”  $(\bar{g}_{\mu\nu}, \bar{\phi})$  is a solution of Horndeski theory, the disformally transformed solution  $(g_{\mu\nu}, \phi)$  is a solution of the *beyond Horndeski* theory [182].

In our analysis [179], we chose to consider as our “seed” solution  $(\bar{g}_{\mu\nu}, \bar{\phi})$  the static, spherically-symmetric solution (56). Since  $\phi = \phi(r)$ , the disformal transformation will result in the relations

$$h = \bar{h}, \quad f = \frac{\bar{f}}{1 + 2D\bar{X}} \equiv \bar{f}W(\bar{X}), \quad (65)$$

where, for convenience, we have defined a new arbitrary function  $W(\bar{X})$ . There is clearly an arbitrarily large number of choices for the function  $D(\bar{X})$  or  $W(\bar{X})$ . Its form will be dictated by the desired properties of the new metric tensor. For instance, it is clear that  $W(\bar{X})$  should satisfy the following two constraints

$$W(\bar{X}) \geq 0, \quad \lim_{r \rightarrow \infty} W(\bar{X}) = 1, \quad (66)$$

in order to preserve the signature and asymptotic behaviour of  $\bar{g}_{\mu\nu}$ . In addition, in order to obtain a spacetime with a throat, we allowed the existence of a root

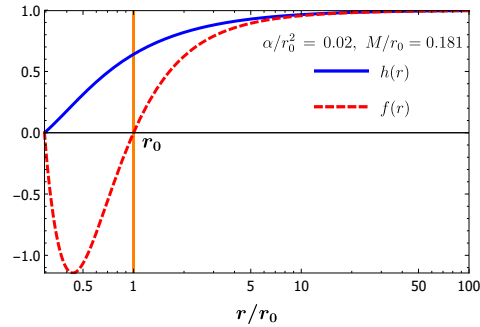


**Fig. 10.** The two metric functions after the disformal transformation [179].

in the expression of  $W(\bar{X})$  at a distance  $r_0 > r_H$ , where  $r_H$  is the event horizon of the “seed solution”. The presence of this root would result into the vanishing of  $g^{rr}$  at this point but not of  $g_{tt}$ , which will remain a constant. This is indeed the typical behaviour of the metric tensor close to a wormhole according to the discussion in Section 3.2. For example, we could choose [179]

$$W(\bar{X}) = 1 - \frac{r_0}{\lambda} \sqrt{-2\bar{X}} = 1 - \frac{r_0}{\lambda r} (1 - \sqrt{h}) , \quad (67)$$

where  $\lambda$  is a scale parameter of the solution. The root  $r_0$ , or the radius of the wormhole, is located at

$$r_0 = \frac{M \pm \sqrt{M^2 - \alpha\lambda^3(2-\lambda)^3}}{\lambda(2-\lambda)} , \quad (68)$$

and is determined by the mass  $M$  of the original black-hole solution, the coupling parameter  $\alpha$  and the scalar parameter  $\lambda$ . The profiles of the two metric functions  $h(r)$  and  $f(r)$  after the disformal transformation are depicted in Fig. 10.

Due to the vanishing of the metric function  $f(r)$  at the throat, we focus on the causal part of the spacetime with  $r_0 \leq r < \infty$ . The complete geometry is revealed by setting  $r^2 = l^2 + r_0^2$ , in which case the line-element reads

$$ds^2 = -H(l) dt^2 + \frac{dl^2}{F(l)} + (l^2 + r_0^2) d\Omega^2 , \quad (69)$$

where

$$H(l) = h(r(l)) , \quad F(l) = \frac{f(r(l))(l^2 + r_0^2)}{l^2} . \quad (70)$$

The throat of the wormhole is now located at  $l = 0$  and the two asymptotic regimes are reached when  $l \rightarrow \pm\infty$ . The two metric functions  $H(l)$  and  $F(l)$  are everywhere regular and they both assume constant values at the throat. Their profiles are depicted in Fig. 11. We observe that both metric functions are symmetric under the change  $l \rightarrow -l$  and that their first derivatives vanish at the

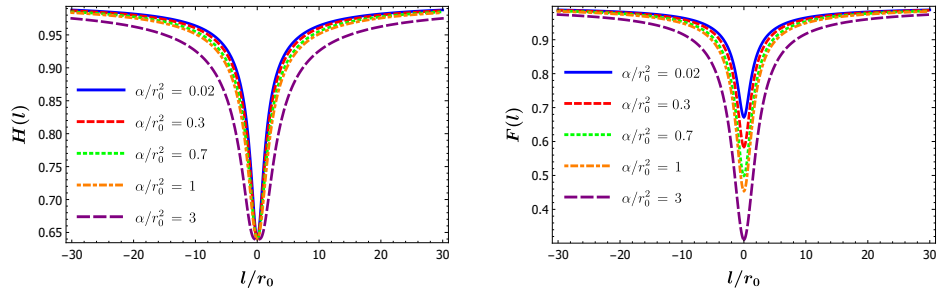


**Fig. 11.** The two metric functions after the change of variable  $r \rightarrow l$  [179].

throat (all curves in Fig. 11 become horizontal there). As a result, no cusp points appear at the throat and the two parts of the wormhole (the positive and negative  $l$ -regimes) are smoothly connected. The wormhole is therefore traversable without the need of any distribution of additional matter, exotic or not.

The spacetime is everywhere regular and smooth, and this is evident in the form of the Kretschmann scalar  $\mathcal{K} = R^{\mu\nu\rho\sigma} R_{\mu\nu\rho\sigma}$  presented on the left plot of Fig. 12. We also observe that the non-vanishing curvature is restricted in a narrow region  $-2r_0 \leq l \leq 2r_0$  thus our wormholes may comprise ultra-compact objects. One could construct the embedding diagram of the solution by following a procedure similar to that of Section 3.2. Although the details differ, the embedding diagram presents exactly the same form as the one shown in Fig. 5. The profile of the scalar field is depicted on the right plot; this in fact asymmetric under the change  $l \rightarrow -l$ , but is again regular over the entire regime and presents no discontinuities.

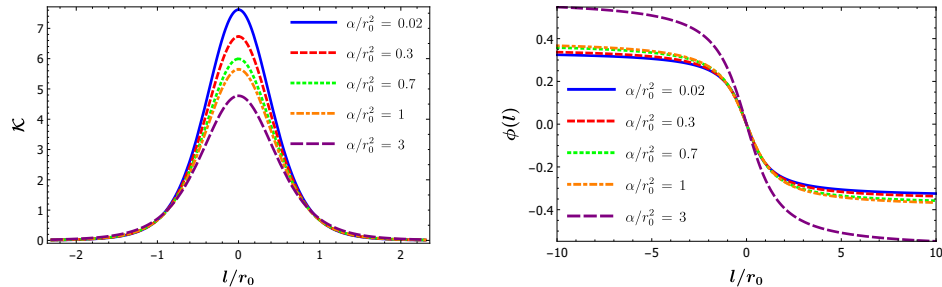


**Fig. 12.** The Kretschmann scalar  $\mathcal{K}$  (left plot), and the profile of the scalar field (right plot) [179].

One may wonder whether the emergence of these wormhole solutions must again be supported by the violation of the energy conditions. If we focus again

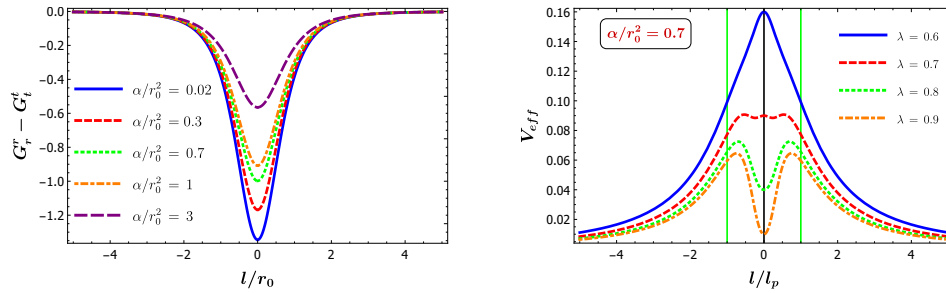


**Fig. 13.** The violation of the NEC (left plot) and the effective potential of photons propagating in the wormhole background (right plot) [179].

on the Null Energy Condition, namely  $T_{\mu\nu}n^\mu n^\nu \geq 0$ , we arrive at the result

$$8\pi G(T_r^r - T_t^t) = G_r^r - G_t^t = -\frac{f'(r_0)}{r_0}. \quad (71)$$

But one may easily see that the condition  $f'(r_0) < 0$  is the flaring-out condition for these wormholes and thus must be always respected. As a result, the NEC is again violated, as one may see also on the left plot of Fig. 13. But this violation is again caused not by the presence of any exotic matter but by the various non-minimal couplings of the scalar field to gravity in this theory. What is also important is that the energy-density  $\rho$  of the theory for most of the solutions is everywhere positive which renders our solutions more physically interesting and realistic.

Turning finally to observable phenomena that one could associate with our wormhole solutions, we address again the geodesics of null particles as an indicative example. These are given by the equation

$$Wr'^2 + \frac{h}{r^2} = \frac{E^2}{L^2}. \quad (72)$$

Studying the extremal points of the photon's effective potential  $V_{eff} = h/r^2$ , we find that these are given by the 3rd-order polynomial

$$r^3 - 9M^2r + 8\alpha M = 0. \quad (73)$$

As expected, in the limit  $\alpha \rightarrow 0$ , we obtain two extremal points at  $r = 0$  and  $r = 3M$ , with the first one being stable and the second unstable. As  $\alpha$  increases, we find up to 3 extremal points, one at the throat and two more at larger radii. In this case, the light ring around the throat and the more distant one are stable while the intermediate one is unstable; all light rings lie at distances smaller than  $3M$ , which is the characteristic light-ring radius of the Schwarzschild spacetime. The effective potential for null particles is depicted on the right plot of Fig. 13.

## 5 Conclusions

In the quest of new black-hole solutions, traversable wormholes and regular particle-like solutions, one is forced to move beyond General Relativity and to consider generalised theories of gravity. Scalar-tensor theories is the simplest extension of GR, however, one must consider non-minimally coupled scalar fields in order for physically-interesting solutions to emerge. The Einstein-scalar-Gauss-Bonnet theory is an indicative example of such a theory that contains a single scalar degree of freedom coupled to the quadratic, gravitational Gauss-Bonnet term, a term which is bound to lead to important modifications from GR in the strong-gravity regime. It was in the context of this theory that we sought for new solutions describing compact objects and being characterized by a non-trivial scalar field.

We demonstrated that the EsGB theory admits a variety of solutions. Scalarised black-hole solutions were discovered first for particular forms of the coupling function between the scalar field and the GB term. In the recent years, it was demonstrated that scalarised, black-hole solutions with a regular horizon and a Minkowski or Anti-de Sitter behaviour at large distances always emerge, independently of the form of the coupling function, provided that appropriate boundary conditions are imposed. These black-hole solutions evade all known forms of the scalar no-hair theorem as the presence of the GB term causes the violation of the theorem's requirements.

Similar analyses for the determination of wormhole solutions soon followed based on the common knowledge that the GB term violates the energy conditions, a requirement for the emergence of a traversable wormhole. Indeed, a plethora of wormhole solutions were found for various forms of the coupling function of the scalar field to the GB term. In order to avoid a spacetime singularity lurking somewhere behind the throat, a cut & paste technique was applied which smoothly connected two regular regimes thus creating a traversable wormhole with a regular scalar field. The study of particle geodesics in this background showed that trajectories starting from one side of the wormhole, crossing the throat, visiting the other side of the wormhole and then returning back to the departure point was a common behaviour.

Gravitational, particle-like solutions were also studied in the context of the EsGB theory causing perhaps no surprise when such solutions readily emerged for various forms of the coupling function. A singularity seemed to plague the expression of the scalar field, however, it was found that this has no physical consequence for the spacetime curvature, energy-momentum tensor or particle trajectories, thus rendering this singularity a harmless, "Coulomb-type" singularity. These regular, particle-like solutions presented a bubble-type distribution of matter with a negative value of energy density at the center, a positive value at the peak of the distribution located very close to the origin and a fast decreasing profile - the latter features render our solutions as ultra-compact objects. The study of null particles in the background of the more compact solutions revealed the existence of a pair of light-rings, an inner stable one and an outer unstable. The study of a scalar field propagating in the same spacetime led to the

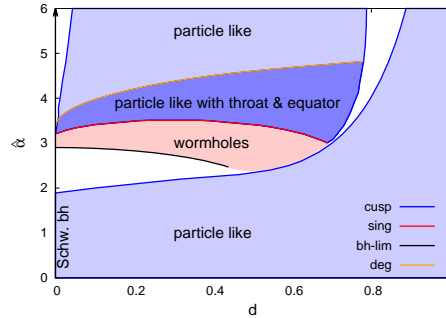


**Fig. 14.** The different types of solutions emerging in the context of the Einstein-scalar-GB theory [166][167].

result that a series of echoes should characterize the wave signal at infinity, a characteristic observable associated to our particle-like solutions.

The different types of solutions emerging in the context of the EsGB theory are depicted in the domain-of-existence plot of Fig. 14. In there, we may see the line of scalarised black-hole solutions, a one-parameter family of solutions due to the no-hair theorem which acts as a boundary of the wormhole territory. The latter solutions may be characterised by a single throat or by a pair of throats with an equator in between. In the same plot, we also notice different families of particle-like solutions, characterised by an increasing number of nodes of the scalar field as the coupling constant of the theory increases, too. We also observe that some white, uncharted yet, areas still remain in the domain of existence which creates perhaps expectations for future discoveries!

The transition from General Relativity to the Einstein-scalar-Gauss-Bonnet theory resulted in the discovery of a wealth of solutions which, in the former theory, were forbidden. The EsGB theory itself is a subclass of Horndeski theory, which is a much more general scalar-tensor theory characterized by four coupling functions. Although more complicated, the set of field equations can be rendered integrable upon appropriate choices for the four coupling functions. The theory can be further generalised to the beyond-Horndeski theory via the addition of two additional terms in the Lagrangian. In the context of this latter theory, we re-examined the integrability of the set of field equations, formulated these in a particularly convenient form, and investigated the existence of analytical solutions describing black holes. In the context of the parity-symmetric sector of the theory, we analytically determined a large number of black-hole solutions with an (Anti-)de Sitter-Reissner-Nordstrom asymptotic behaviour at large distances. In the case of parity-symmetry breaking, the determination of analytic solutions in a closed form is much more difficult.

Turning to the family of wormhole solutions, we chose to determine these not by analytically solving the field equations but by applying a disformal transformation to a known, “seed”, solution of the theory. That was made possible

by conveniently choosing the function of the disformal transformation. The resulting wormhole solutions were shown to be generically regular by construction, localised in a very narrow range of the radial coordinate – a feature which renders our solutions as ultra-compact objects – and to be characterised by a non-trivial scalar field. Studying the particle trajectories in the wormhole spacetime, distinct observable signatures were determined such as the emergence of multiple photon rings, some of them stable and all located at radii smaller than the characteristic distance of  $3M$  of the Schwarzschild solution.

Due to the larger arbitrariness of the Horndeski and beyond-Horndeski theories, encoded in the forms of the four and six, respectively, undetermined a priori coupling functions, the phase-space of the solutions of the theory has not yet fully been studied. Specific sectors have been studied for particular classes of solutions but the study of the complete theory as well as the charting of the types of solutions that the theory harbors is still lacking. Judging by the variety of solutions that have so far been found and by the wealth of solutions arising in the context of the EsGB theory, which is only a subclass of the theory, we expect a great many discoveries – even surprises – to arise when the complete Horndeski and beyond Horndeski theories are fully investigated.

**Acknowledgements.** I am grateful to my collaborators Georgios Antoniou, Athanasios Bakopoulos, Christos Charmousis, Nicolas Lecoer, Burkhard Kleihaus, Jutta Kunz and Nikolaos Pappas for our enjoyable and fruitful collaboration. I am also deeply thankful to the organisers of the 11th Aegean Summer School for their kind invitation and for giving me the opportunity to present our results.

## References

1. A. Einstein, Sitzungsber. Preuss. Akad. Wiss. Berlin (Math. Phys. ) **1915** (1915), 844-847; Sitzungsber. Preuss. Akad. Wiss. Berlin (Math. Phys. ) **1915** (1915), 831-839; Sitzungsber. Preuss. Akad. Wiss. Berlin (Math. Phys. ) **1915** (1915), 778-786; Annalen Phys. **49** (1916) no.7, 769-822.
2. K. A. Bronnikov, Acta Phys. Polon. B **4** (1973), 251-266
3. K. S. Stelle, Phys. Rev. D **16** (1977) 953.
4. T. P. Sotiriou, Lect. Notes Phys. **892** (2015) 3.
5. E. Berti *et al.*, Class. Quant. Grav. **32** (2015) 243001.
6. C. Charmousis, Lect. Notes Phys. **769** (2009) 299; Lect. Notes Phys. **892** (2015), 25-56.
7. C. G. Callan, Jr., I. R. Klebanov and M. J. Perry, Nucl. Phys. B **278** (1986), 78-90.
8. D. J. Gross and J. H. Sloan, Nucl. Phys. B **291** (1987), 41-89.
9. R. R. Metsaev and A. A. Tseytlin, Nucl. Phys. B **293** (1987), 385-419.
10. D. Lovelock, J. Math. Phys. **12** (1971), 498-501.
11. G. W. Horndeski, Int. J. Theor. Phys. **10** (1974), 363-384.
12. K. Schwarzschild, Sitzungsber. Preuss. Akad. Wiss. Berlin (Math. Phys. ) **1916** (1916), 189-196; Sitzungsber. Preuss. Akad. Wiss. Berlin (Math. Phys. ) **1916** (1916), 424-434.
13. H. Reissner, Annalen der Physik 50 (9) (1916), 106–120; G. Nordström, Verhandl. Koninkl. Ned. Akad. Wetenschap., Afdel. Natuurk., Amsterdam. **26** (1918), 1201–1208.

14. R. P. Kerr, *Phys. Rev. Lett.* **11** (1963), 237-238.
15. J. D. Bekenstein, *Phys. Rev. Lett.* **28** (1972) 452; C. Teitelboim, *Lett. Nuovo Cim.* **3S2** (1972) 397.
16. C. A. R. Herdeiro and E. Radu, *Int. J. Mod. Phys. D* **24** (2015) no.09, 1542014.
17. C. W. Misner, K. S. Thorne and J. A. Wheeler, W. H. Freeman, 1973, ISBN 978-0-7167-0344-0, 978-0-691-17779-3
18. A. Einstein and N. Rosen, *Phys. Rev.* **48** (1935), 73-77.
19. C. W. Misner and J. A. Wheeler, *Annals Phys.* **2** (1957), 525-603.
20. M. Visser, "Lorentzian wormholes: From Einstein to Hawking," *Computational and Mathematical Physics*, American Inst. of Physics, 1995.
21. M. S. Morris and K. S. Thorne, *Am. J. Phys.* **56** (1988), 395-412.
22. H. G. Ellis, *Journal of Math. Physics.* **14** (1973), 104-118.
23. K. A. Bronnikov, *Acta Physica Polonica.* **B4** (1973), 251-266.
24. I. Fisher, *Zh. Eksp. Teor. Fiz.* **18** (1948), 636.
25. A. I. Janis, E. T. Newman, and J. Winicour, *Phys. Rev. Lett.* **20** (1968), 878.
26. M. Wyman, *Phys. Rev. D* **24** (1981), 839.
27. H. Motohashi and T. Suyama, *Phys. Rev. D* **91** (2015), 085009.
28. P. Kanti, N. E. Mavromatos, J. Rizos, K. Tamvakis and E. Winstanley, *Phys. Rev. D* **54** (1996) 5049;
29. P. Kanti, N. E. Mavromatos, J. Rizos, K. Tamvakis and E. Winstanley, *Phys. Rev. D* **57** (1998) 6255.
30. G. W. Gibbons and K. i. Maeda, *Nucl. Phys. B* **298** (1988) 741.
31. C. G. Callan, Jr., R. C. Myers and M. J. Perry, *Nucl. Phys. B* **311** (1989) 673.
32. B. A. Campbell, M. J. Duncan, N. Kaloper and K. A. Olive, *Phys. Lett. B* **251** (1990) 34; B. A. Campbell, N. Kaloper and K. A. Olive, *Phys. Lett. B* **263** (1991) 364.
33. S. Mignemi and N. R. Stewart, *Phys. Rev. D* **47** (1993) 5259.
34. P. Kanti and K. Tamvakis, *Phys. Rev. D* **52** (1995) 3506.
35. T. Torii, H. Yajima and K. i. Maeda, *Phys. Rev. D* **55** (1997) 739.
36. P. Kanti and K. Tamvakis, *Phys. Lett. B* **392** (1997) 30.
37. Z. K. Guo, N. Ohta and T. Torii, *Prog. Theor. Phys.* **120** (2008) 581; N. Ohta and T. Torii, *Prog. Theor. Phys.* **122** (2009) 1477; K. i. Maeda, N. Ohta and Y. Sasagawa, *Phys. Rev. D* **80** (2009) 104032; N. Ohta and T. Torii, *Prog. Theor. Phys.* **124** (2010) 207.
38. B. Kleihaus, J. Kunz and E. Radu, *Phys. Rev. Lett.* **106** (2011) 151104; B. Kleihaus, J. Kunz, S. Mojica and E. Radu, *Phys. Rev. D* **93** (2016) no.4, 044047.
39. P. Pani, C. F. B. Macedo, L. C. B. Crispino and V. Cardoso, *Phys. Rev. D* **84** (2011) 087501; P. Pani, E. Berti, V. Cardoso and J. Read, *Phys. Rev. D* **84** (2011) 104035.
40. Y. Bardoux, M. M. Caldarelli and C. Charmousis, *JHEP* **1205** (2012) 054.
41. K. Yagi, L. C. Stein, N. Yunes and T. Tanaka, *Phys. Rev. D* **85** (2012) 064022 Erratum: [*Phys. Rev. D* **93** (2016) no.2, 029902].
42. C. Charmousis, T. Kolyvaris, E. Papantonopoulos and M. Tsoukalas, *JHEP* **1407** (2014) 085.
43. F. Correa, M. Hassaine and J. Oliva, *Phys. Rev. D* **89** (2014) no.12, 124005.
44. D. Ayzenberg and N. Yunes, *Phys. Rev. D* **90** (2014) 044066 Erratum: [*Phys. Rev. D* **91** (2015) no.6, 069905].
45. J. L. Blazquez-Salcedo, C. F. B. Macedo, V. Cardoso, V. Ferrari, L. Gualtieri, F. S. Khoo, J. Kunz and P. Pani, *Phys. Rev. D* **94** (2016) no.10, 104024.
46. S. Bhattacharya and S. Chakraborty, *Phys. Rev. D* **95** (2017) no.4, 044037; I. Banerjee, S. Chakraborty and S. SenGupta, *Phys. Rev. D* **96** (2017) no.8, 084035.



47. J. L. Blazquez-Salcedo *et al.*, IAU Symp. **324** (2016) 265.
48. T. P. Sotiriou and S. Y. Zhou, Phys. Rev. Lett. **112** (2014) 251102.
49. T. P. Sotiriou and S. Y. Zhou, Phys. Rev. D **90** (2014) 124063; R. Benkel, T. P. Sotiriou and H. Witek, Phys. Rev. D **94** (2016) no.12, 121503; Class. Quant. Grav. **34** (2017) no.6, 064001.
50. J. D. Bekenstein, Phys. Rev. D **51** (1995) no.12, R6608.
51. T. P. Sotiriou and V. Faraoni, Phys. Rev. Lett. **108** (2012) 081103.
52. L. Hui and A. Nicolis, Phys. Rev. Lett. **110** (2013) 241104.
53. C. A. R. Herdeiro and E. Radu, Phys. Rev. Lett. **112** (2014) 221101.
54. E. Babichev and C. Charmousis, JHEP **1408** (2014) 106.
55. G. Antoniou, A. Bakopoulos and P. Kanti, Phys. Rev. Lett. **120** (2018) no.13, 131102.
56. G. Antoniou, A. Bakopoulos and P. Kanti, Phys. Rev. D **97** (2018) no.8, 084037.
57. A. Papageorgiou, C. Park and M. Park, Phys. Rev. D **106** (2022) no.8, 084024.
58. A. Bakopoulos, G. Antoniou and P. Kanti, Phys. Rev. D **99** (2019) no.6, 064003.
59. Y. Brihaye, B. Hartmann and J. Urrestilla, JHEP **1806** (2018) 074; Y. Brihaye and B. Hartmann, arXiv:1810.05108 [gr-qc].
60. Y. Brihaye and B. Hartmann, Phys. Lett. B **772** (2017), 476-482
61. A. Bakopoulos, P. Kanti and N. Pappas, Phys. Rev. D **101** (2020) no.8, 084059
62. D. D. Doneva and S. S. Yazadjiev, Phys. Rev. Lett. **120** (2018) no.13, 131103.
63. H. O. Silva, J. Sakstein, L. Gualtieri, T. P. Sotiriou and E. Berti, Phys. Rev. Lett. **120** (2018) no.13, 131104.
64. D. D. Doneva and S. S. Yazadjiev, JCAP **1804** (2018) no.04, 011.
65. H. Motohashi and M. Minamitsuji, Phys. Lett. B **781** (2018) 728; Phys. Rev. D **98** (2018) no.8, 084027.
66. C. A. R. Herdeiro, E. Radu, N. Sanchis-Gual and J. A. Font, Phys. Rev. Lett. **121** (2018) no.10, 101102; T. Delsate, C. Herdeiro and E. Radu, Phys. Lett. B **787** (2018) 8; Y. Brihaye, C. Herdeiro and E. Radu, Phys. Lett. B **788** (2019) 295.
67. D. D. Doneva, S. Kiorpelidi, P. G. Nedkova, E. Papantonopoulos and S. S. Yazadjiev, Phys. Rev. D **98** (2018) no.10, 104056.
68. M. Butler, A. M. Ghezelbash, E. Massaeli and M. Motaharfar, arXiv:1808.03217 [hep-th].
69. B. Danila, T. Harko, F. S. N. Lobo and M. K. Mak, arXiv:1811.02742 [gr-qc].
70. M. M. Stetsko, arXiv:1811.05030 [hep-th].
71. O. J. Tattersall, P. G. Ferreira and M. Lagos, Phys. Rev. D **97** (2018) no.8, 084005.
72. S. Mukherjee and S. Chakraborty, Phys. Rev. D **97** (2018) no.12, 124007.
73. S. Chakrabarti, Eur. Phys. J. C **78** (2018) no.4, 296.
74. E. Berti, K. Yagi and N. Yunes, Gen. Rel. Grav. **50** (2018) no.4, 46.
75. Y. Brihaye and B. Hartmann, Class. Quant. Grav. **35** (2018) no.17, 175008.
76. K. Prabhu and L. C. Stein, Phys. Rev. D **98** (2018) no.2, 021503.
77. Y. S. Myung and D. C. Zou, Phys. Rev. D **98** (2018) no.2, 024030; arXiv:1812.03604 [gr-qc].
78. J. L. Blazquez-Salcedo, D. D. Doneva, J. Kunz and S. S. Yazadjiev, Phys. Rev. D **98** (2018) no.8, 084011; J. L. Blazquez-Salcedo, Z. Altaha Motahar, D. D. Doneva, F. S. Khoo, J. Kunz, S. Mojica, K. V. Staykov and S. S. Yazadjiev, arXiv:1810.09432 [gr-qc].
79. R. Benkel, N. Franchini, M. Saravani and T. P. Sotiriou, Phys. Rev. D **98** (2018) no.6, 064006.
80. B. H. Lee, W. Lee and D. Ro, Phys. Rev. D **99** (2019) no.2, 024002.
81. H. Witek, L. Gualtieri, P. Pani and T. P. Sotiriou, Phys. Rev. D **99** (2019) no.6, 064035.

82. H. Motohashi and S. Mukohyama, Phys. Rev. D **99** (2019) no.4, 044030.
83. J. Sultana and D. Kazanas, Gen. Rel. Grav. **50** (2018) no.11, 137.
84. S. Nojiri, S. D. Odintsov and V. K. Oikonomou, Phys. Rev. D **99** (2019) 044050.
85. S. Qolibikloo and A. Ghodsi, Eur. Phys. J. C **79** (2019) no.5, 406.
86. P. V. P. Cunha, C. A. R. Herdeiro and E. Radu, Phys. Rev. Lett. **123**, no. 1, 011101 (2019).
87. A. Bakopoulos, P. Kanti and N. Pappas, Phys. Rev. D **101** (2020) no.4, 044026.
88. M. Minamitsuji and T. Ikeda, Phys. Rev. D **99** (2019) 044017; Phys. Rev. D **99** (2019) 104069.
89. M. M. Stetsko, Phys. Rev. D **99** (2019) 044028.
90. Y. S. Myung and D.-C. Zou, Phys. Lett. B **790** (2019) 400.
91. Y. Brihaye and L. Ducobu, Phys. Lett. B **795** (2019) 135.
92. C. A. R. Herdeiro and E. Radu, Phys. Rev. D **99** (2019) 084039.
93. T. Kobayashi, Rept. Prog. Phys. **82** (2019) 086901.
94. H. O. Silva, C. F. B. Macedo, T. P. Sotiriou, L. Gualtieri, J. Sakstein and E. Berti, Phys. Rev. D **99** (2019) 104041.
95. A. de la Cruz-Dombriz and F. J.M. Torralba, JCAP **1903** (2019) 002.
96. C.-Y. Wang, Y.-F. Shen and Y. Xie, JCAP **1904** (2019) 022.
97. P.-A. Cano and A. Ruiperez, JHEP **1905** (2019) 189.
98. F. M. Ramazanoglu, Phys. Rev. D **99** (2019) 084015.
99. P. G. S. Fernandes, C. A. R. Herdeiro, A. M. Pombo, E. Radu and N. Sanchis-Gual, Class. Quant. Grav. **36** (2019) 134002.
100. Y. Brihaye and B. Hartmann, Phys. Lett. B **792** (2019) 244.
101. M. Saravani and T. P. Sotiriou, Phys. Rev. D **99** (2019) 124004.
102. C. F. B. Macedo, J. Sakstein, E. Berti, L. Gualtieri, H. O. Silva and T. P. Sotiriou, Phys. Rev. D **99** (2019) 104041.
103. D. D. Doneva, K. V. Staykov and S. S. Yazadjiev, Phys. Rev. D **99** (2019) 104045.
104. A. Saffer, H. O. Silva and N. Yunes, Phys. Rev. D **100** (2019) 044030.
105. T. Anson, E. Babichev, C. Charmousis and S. Ramazanov, JCAP **1906** (2019) 023.
106. Y. S. Myung and D.-C. Zou, Int. J. Mod. Phys. D **28** (2019) 1950114.
107. Y. Brihaye and B. Hartmann, JHEP **1909** (2019) 049.
108. O. J. Tattersall and P. G. Ferreira, Phys. Rev. D **99** (2019) 104082.
109. N. Andreou, N. Franchini, G. Ventagli and T. P. Sotiriou, Phys. Rev. D **99** (2019) 124022.
110. Q. Liang, J. Sakstein and M. Trodden, Phys. Rev. D **100** (2019) 063518.
111. L. Hui, D. Kabat, X. Li, L. Santoni and S. S. C. Wong, JCAP **1906** (2019) 038.
112. D. Q. Tuan and S. H. Q. Nguyen, Commun. Phys. **29** (2019) 173.
113. Tuan Do *et al*, Science **365** (2019) 6454.
114. P. G. S. Fernandes, C. A. R. Herdeiro, A. M. Pombo, E. Radu and N. Sanchis-Gual, Phys. Rev. D **100** (2019) 084045.
115. R. A. Konoplya and A. Zhidenko, Phys. Rev. D **100** (2019) 044015.
116. N. Franchini and T. P. Sotiriou, arXiv:1903.05427 [gr-qc].
117. A. Hees, O. Minazzoli, E. Savalle, Y. V. Stadnik, P. Wolf and B. Roberts, arXiv:1905.08524 [gr-qc].
118. T. Anson, E. Babichev and S. Ramazanov, arXiv:1905.10393 [gr-qc].
119. C. Charmousis, M. Crisostomi, R. Gregory and N. Stergioulas, Phys. Rev. D **100** (2019) no.8, 084020
120. M. Khalil, N. Sennett, J. Steinhoff and A. Buonanno, arXiv:1906.08161 [gr-qc].
121. C. de Rham and J. Zhang, arXiv:1907.006992 [hep-th].

122. G. Aguilar-Perez, M. Cruz, S. Lepe and I. Moran-Rivera, arXiv:1907.06168 [gr-qc].
123. R. A. Konoplya, T. Pappas and A. Zhidenko, arXiv:1907.10112 [gr-qc].
124. Y.-X. Gao and D.-J. Liu, arXiv:1908.01346 [gr-qc].
125. T. Ikeda, T. Nakamura and M. Minamitsuji, arXiv:1908.09394 [gr-qc].
126. F.-L. Julie and E. Berti, arXiv:1909.05258 [gr-qc].
127. F. M. Ramazanoglu and K. I. Unluturk, arXiv:1910.02801 [gr-qc].
128. K. V. Aelst, E. Gourgoulhon, P. Grandclement and C. Charmousis, arXiv:1910.08451 [gr-qc].
129. J. Barrientos, F. Cordonier-Tello, C. Corral, F. Izaurieta, P. Medina, E. Rodriguez and O. Valdivia, arXiv:1910.00148 [gr-qc].
130. C. Martinez, R. Troncoso and J. Zanelli, Phys. Rev. D **67** (2003) 024008.
131. T. J. T. Harper, P. A. Thomas, E. Winstanley and P. M. Young, Phys. Rev. D **70** (2004) 064023.
132. T. Torii, K. Maeda and M. Narita, Phys. Rev. D **59** (1999) 064027.
133. E. Winstanley, Found. Phys. **33** (2003) 111; Class. Quant. Grav. **22** (2005) 2233.
134. S. Bhattacharya and A. Lahiri, Phys. Rev. Lett. **99** (2007) 201101.
135. M. Henneaux, C. Martinez, R. Troncoso and J. Zanelli, Phys. Rev. D **70** (2004) 044034; C. Martinez, R. Troncoso and J. Zanelli, Phys. Rev. D **70** (2004) 084035; C. Erices and C. Martinez, Phys. Rev. D **97** (2018) no.2, 024034.
136. E. Radu and E. Winstanley, Phys. Rev. D **72** (2005) 024017.
137. A. Anabalón and H. Maeda, Phys. Rev. D **81** (2010) 041501.
138. D. Hosler and E. Winstanley, Phys. Rev. D **80** (2009) 104010.
139. C. Charmousis, T. Kolyvaris and E. Papantonopoulos, Class. Quant. Grav. **26** (2009) 175012; T. Kolyvaris, G. Koutsoumbas, E. Papantonopoulos and G. Siopsis, Gen. Rel. Grav. **43** (2011) 163.
140. K. i. Maeda, N. Ohta and Y. Sasagawa, Phys. Rev. D **83** (2011) 044051; Z. K. Guo, N. Ohta and T. Torii, Prog. Theor. Phys. **121** (2009) 253; N. Ohta and T. Torii, Prog. Theor. Phys. **121** (2009) 959; N. Ohta and T. Torii, Prog. Theor. Phys. **122** (2009) 1477.
141. S. G. Saenz and C. Martinez, Phys. Rev. D **85** (2012) 104047.
142. M. M. Caldarelli, C. Charmousis and M. Hassaine, JHEP **1310** (2013) 015.
143. P. A. Gonzalez, E. Papantonopoulos, J. Saavedra and Y. Vasquez, JHEP **1312** (2013) 021.
144. M. Bravo Gaete and M. Hassaine, Phys. Rev. D **88** (2013) 104011; M. Bravo Gaete and M. Hassaine, JHEP **1311** (2013) 177.
145. G. Giribet, M. Leoni, J. Oliva and S. Ray, Phys. Rev. D **89** (2014) no.8, 085040.
146. J. Ben Achour and H. Liu, arXiv:1811.05369 [gr-qc].
147. J. B. Achour and H. Liu, Phys. Rev. D **99** (2019) 064042.
148. P. Kanti, A. Bakopoulos and N. Pappas, PoS CORFU2018 (2019) 091.
149. Y. Brihaye, C. Herdeiro and E. Radu, arXiv:1910.05286 [gr-qc].
150. D. D. Doneva, K. V. Staykov and S. S. Yazadjiev, Phys. Rev. D **99** (2019) no.10, 104045.
151. Y. Brihaye, C. Herdeiro and E. Radu, Phys. Lett. B **802** (2020) 135269.
152. P. Kanti, B. Kleihaus and J. Kunz, Phys. Rev. Lett. **107** (2011), 271101.
153. P. Kanti, B. Kleihaus and J. Kunz, Phys. Rev. D **85** (2012), 044007.
154. G. Antoniou, A. Bakopoulos, P. Kanti, B. Kleihaus and J. Kunz, Phys. Rev. D **101** (2020) no.2, 024033.
155. K. A. Bronnikov and J. C. Fabris, Class. Quant. Grav. **14** (1997), 831-842.
156. F. S. N. Lobo, Phys. Rev. D **71** (2005), 084011.

157. S. V. Bolokhov, K. A. Bronnikov and M. V. Skvortsova, *Class. Quant. Grav.* **29** (2012), 245006.
158. B. Kleihaus and J. Kunz, *Phys. Rev. D* **90**, 121503 (2014).
159. M. R. Mehdizadeh, M. Kord Zangeneh and F. S. N. Lobo, *Phys. Rev. D* **91** (2015) no.8, 084004.
160. K. A. Bronnikov, J. C. Fabris, O. F. Piattella and E. C. Santos, *Gen. Rel. Grav.* **48** (2016) no.12, 162
161. R. Shaikh and S. Kar, *Phys. Rev. D* **94** (2016) no.2, 024011
162. P. Cañate, J. Sultana and D. Kazanas, *Phys. Rev. D* **100** (2019) no.6, 064007
163. K. A. Bronnikov, S. V. Bolokhov and M. V. Skvortsova, *Int. J. Mod. Phys. D* **28** (2019) no.13, 1941008.
164. R. Ibadov, B. Kleihaus, J. Kunz and S. Murodov, *Phys. Rev. D* **102** (2020) no.6, 064010.
165. R. Ibadov, B. Kleihaus, J. Kunz and S. Murodov, *Symmetry* **13** (2021) no.1, 89.
166. B. Kleihaus, J. Kunz and P. Kanti, *Phys. Lett. B* **804** (2020), 135401.
167. B. Kleihaus, J. Kunz and P. Kanti, *Phys. Rev. D* **102** (2020), 024070.
168. V. Cardoso, L. C. B. Crispino, C. F. B. Macedo, H. Okawa and P. Pani, *Phys. Rev. D* **90** (2014) no.4, 044069
169. J. Keir, *Class. Quant. Grav.* **33** (2016) no.13, 135009.
170. P. Cunha, V.P., E. Berti and C. A. R. Herdeiro, *Phys. Rev. Lett.* **119** (2017) no.25, 251102.
171. Y. Brihaye and B. Hartmann, *JHEP* **09** (2019), 049.
172. H. Lu and Y. Pang, *Phys. Lett. B* **809** (2020), 135717.
173. R. A. Hennigar, D. Kubizňák, R. B. Mann and C. Pollack, *JHEP* **07** (2020), 027.
174. J. Ben Achour, M. Crisostomi, K. Koyama, D. Langlois, K. Noui and G. Tasinato, *JHEP* **12** (2016), 100.
175. A. Bakopoulos, C. Charmousis, P. Kanti and N. Lecoeur, *JHEP* **08** (2022), 055.
176. E. Babichev, C. Charmousis and A. Lehébel, *Class. Quant. Grav.* **33** (2016) no.15, 154002.
177. E. Babichev, C. Charmousis and A. Lehébel, *JCAP* **04** (2017), 027.
178. E. Babichev, C. Charmousis, M. Hassaine and N. Lecoeur, *Phys. Rev. D* **108** (2023) no.2, 024019.
179. A. Bakopoulos, C. Charmousis and P. Kanti, *JCAP* **05** (2022) no.05, 022.
180. N. Chatzifotis, E. Papantonopoulos and C. Vlachos, *Phys. Rev. D* **105** (2022) no.6, 064025.
181. M. Zumalacárregui and J. García-Bellido, *Phys. Rev. D* **89** (2014), 064046.
182. M. Crisostomi, M. Hull, K. Koyama and G. Tasinato, *JCAP* **03** (2016), 038.
183. J. Ben Achour, M. Crisostomi, K. Koyama, D. Langlois, K. Noui and G. Tasinato, *JHEP* **12** (2016), 100.